National Library of Canada
Acquisitions and Bibliographic Services Branch
395 Wellington Street
Ottawa, Ontario
K1A 0N4

Bibliothèque nationale du Canada
Direction des acquisitions et des services bibliographiques
395, rue Wellington
Ottawa (Ontario)
K1A 0N4

Your file Votre référence

Our file Notre référence

NOTICE

The quality of this microform is heavily dependent upon the quality of the original thesis submitted for microfilming. Every effort has been made to ensure the highest quality of reproduction possible.

If pages are missing, contact the university which granted the degree.

Some pages may have indistinct print especially if the original pages were typed with a poor typewriter ribbon or if the university sent us an inferior photocopy.

AVIS

La qualité de cette microforme dépend grandement de la qualité de la thèse soumise au microfilmage. Nous avons tout fait pour assurer une qualité supérieure de reproduction.

S'il manque des pages, veuillez communiquer avec l'université qui a conféré le grade.

La qualité d'impression de certaines pages peut laisser à désirer, surtout si les pages originales ont été dactylographiées à l'aide d'un ruban usé ou si l'université nous a fait parvenir une photocopie de qualité inférieure.

Canada

Modification and Characterization of Glucose Oxidase Towards the Development of an Enzyme Amplified Amperometric Immunoassay

Line D'Astous

A Thesis

in

The Department

of

Chemistry and Biochemistry

Presented in Partial Fulfilment of Requirements

for the Degree of Master of Science at

Concordia University

Montréal, Québec, Canada

March 1995

ISBN 0-612-01331-6

Canada

Abstract

Modification and Characterization of Glucose Oxidase Towards the Development of an Enzyme Amplified Amperometric Immunoassay

Line D'Astous

In this work, purified glucose oxidase (GOx) was enzymatically deglycosylated using α-mannosidase and endoglycosidase H. Characterization of deglycosylated GOx was carried out by SDS-PAGE and electrospray mass spectrometry, and ~16% mass loss due to deglycosylation was estimated using the latter technique

GOx was covalently modified at lysine residues with 2,4-dinitrobenzoic acid (DNBA) and at aspartic and glutamic acid residues with fluorescein glycine amide (FGA) using carbodiimide and N-hydroxysuccinimide reagents to promote amide bond formation After purification, the FGA product had an average FGA GOx ratio of 5, while the ratio of DNBA to GOx in the DNBA product was not determined Fluorescence measurements under native and denaturing conditions indicated that FGA was indeed covalently bound to GOx Antibody binding to both free and enzyme-bound FGA was studied by fluorescence spectroscopy, and the results showed that free FGA binds more strongly with antibody Electrochemical measurements of GOx activity for $(FGA)_5$-GOx and $(DNBA)_x$-GOx were made in the absence and in the presence of antibody, and only a slight decrease in enzyme activity was observed in the presence of the antibodies The possible use of cyt c as an electron-acceptor substrate for GOx was studied spectrophotometrically as well as electrochemically, using gold electrodes modified with cysteine and 3-mercaptopropionic acid.

Acknowledgements

I would like to thank Professors Ann English and Susan Mikkelsen for their support and guidance throughout my graduate work. I appreciate all their efforts and I am very grateful for their understanding and for having instilled in me the knowledge of Bioanalytical Chemistry.

I would also like to thank Professor Peter Banks for having accepted to serve as a member on my committee and for having proposed helpful ideas during my studies.

A special thank to Bernie Gibbs and George Tsaprailis for all their time and effort with my mass spectrometry experiments and amino acid analysis.

Special thanks to all the people who made this an even more enjoyable experience, George Tsaprailis, Yazhen Hu, Craig Fenwick, Pina Teoli, Ines Holzbaur, Maria Koutroumanis, Haizhi Bu, Kelly Millan, Beata Kolakowski, Angelo Filosa, Salpi Khozozian, Stephen Marmor, Karutha P. Govindaraju and Fernando Battaglini.

Je voudrais aussi remercier une personne très spéciale, mon mari Benoît, pour toute son aide, sa patience et son encouragement. Il est très bon a compter les petits carreaux!

A ma famille et belle-famille, merci d'avoir été si patients et compréhensifs. Bientôt on va pouvoir aller vous voir!

This degree would not have been achieved without the people I have recognized

Table of Content

List of Figures

List of Tables

List of Reactions

List of Abbreviations

Ab	antibody
Ag	antigen
Anti-F	anti-fluoresceinisothiocyanate
Anti-D	anti-dinitrophenol
Asp	aspartic acid
dGOx	deglosylated Gox
dGOx (A)	first sample of deglycosylated GOx
dGOx (B)	second sample of deglycosylated GOx
Cys	cysteine
Cyt c	cytochrome c
DABA	2,4-diaminobenzoic acid
DNBA	2,4-dinitrobenzoic acid
E	enzyme
EDC	1-ethyl-3-(3-dimethylaminopropyl)carbodiiamide
Endo H	endoglycosidase H
FAD	flavin adenine dinucleotide
FCA	ferrocene carboxylic acid
FCOH	ferrocenemethanol
FGA	fluorescein glycine amide
FITC	fluoresceinisothiocyanate
FPLC	fast protein liquid chromatography
GC	gas chromatograph
Glu	glutamic acid
GOx	glucose oxidase
HEPES	4-(2-hydroxyethyl)-1-piperazineethanesulfonic acid
HIC	hydrophobic interaction chromatography
HPLC	high performance liquid chromatography
ES-MS	electrospray mass spectrometry
Lys	lysine
MW	molecular weight
SDS-PAGE	sodium dodecylsulfate polyacrylamide gel electrophoresis
s-NHS	sulfo-N-hydroxysuccinimide
TEMED	tetramethylethylenediamine

1.0 Introduction

Immunoassays are based on the selective binding properties of antibodies, which are large glycoproteins (MW = 150 kD), with antigens or haptens. Haptens are low molecular weight compounds that can only induce an immune response when they are attached to a high molecular weight compound such as a carrier protein. Binding constants as high as 10^{11} have been observed for hapten-antibody binding[1].

Immunoassays provide a sensitive, selective and cost effective method of screening samples, either in the laboratory or directly on-site[2]. Detection and control of environmental pollutants, such as pesticides and industrial chemicals, are important because of their harmful effects. A number of immunoassays have been developed for analysis of small molecules including antibiotics[3], pesticides[4,5], toxins[6], hormones[7], and drugs[8] One advantage of this method over more traditional methods such as gas chromatography (GC) or high performance liquid chromatography (HPLC) is that immunochemical detection is based on the ability of an antibody to act as a receptor for the analyte of interest, and therefore properties such as volatility, thermal stability and chromogenicity are irrelevant. For example, pyrethroid insecticides cannot be easily quantified by GC because they are thermally labile but they can be readily quantified by immunoassay[9]. Currently a lot of work is in progress in the design of haptens specific for the development of pesticide immunoassays[10]. The term enzyme immunoassay describes an immunoassay where the activity of an enzyme is measured to determine the concentration of an analyte.

Glucose oxidase (GOx) is a flavoprotein which catalyses the oxidation of glucose to gluconolactone. It has a carbohydrate content of 16%[11] and possesses 2 flavin adenine

dinucleotide (FAD) centres which are responsible for the redox activity of the enzyme. Since the FAD centres are buried below the surface of GOx[11] (> 13 Å), direct electron transfer between the enzyme and an electrode surface is not observed. Therefore, mediators such as ferrocene derivatives[12] are needed. GOx has been used in immunoassays either as an enzyme-antibody conjugate[13] or an enzyme-hapten conjugate[14].

Modification of GOx with fluorescein glycine amide (FGA) and 2,4-dinitrobenzoic acid (DNBA), and by enzymatic deglycosylation GOx will be presented in Chapter 2. Initial steps towards the development of enzyme amplified amperometric immunoassays using $(FGA)_s$-GOx and $(DNBA)_x$-GOx are discussed in more detail in Chapter 3. In Chapter 4, ferricytochrome c is introduced as an electron-acceptor substrate or mediator for GOx. Chapter 5 presents a summary of the results.

1.1 References

1) Heineman, W R.; Halsall, H.B., Anal. Chem., **1985**, 57, 1321A-1330A.

2) Rittenburg, J H ; Grothaus, G D.; Fitzpatrick, D.A.; Lankow, R.K., Immunoassay for Trace Chemical Analysis, Vanderlaan, M.; Stanker, L.H.; Watkins, L.H.; Roberts, D.W., Ed., ACS Symposium Series 451, **1990**, 28.

3) Yao, R.C ; Mahoney, F.D , J. Antibiotics, **1984**, 37, 1462-1468.

4) van Emon, J.M.; Hammock, B.D ; Seiber, J.N., Anal. Chem., **1985**, 58, 1866-1873.

5) Li, Q.X., Gee, S.J ; McChesney, M.M.; Hammock, B.D.; Seiber, J.N., Anal Chem., **1989**, 61, 819-823.

6) Dixon-Holland, D E.; Pestka, J.J.; Bidigare, B.A.; Casale, W.L.; Warner, R.L ; Ram,

B.P.; Hart, L.P., J. Food. Protection, **1988**, 51, 201-204.

7) Meyer, H.H.D.; Hoffmann, S., Food Additives and Contaminants, **1987**. 4, 149-160.

8) Manning, P.; Athey, D.; McNeil, C.J., Anal. Lett., **1994**, 27, 2443-2453.

9) Stanker, L.H.; Bigbee, C.; van Emon, J.; Watkins, B.E.; Jensen, R.H.; Morris, C.; Vanderlaan, M., J. Agric. Food Chem., **1989**, 37, 834-839.

10) Harrison, R.O.; Goodrow, M.H.; Gee, S.J.; Hammock, B.D., Immunoassay for Trace Chemical Analysis, Vanderlaan, M.; Stanker, L.H.; Watkins, L.H.; Roberts, D.W., Ed., ACS Symposium Series 451, **1990**, 14.

11) Hecht, H.J.; Kalisz, H.M.; Hendle, J.; Schmid, R.D.; Schomburg, D., J. Mol. Biol., **1993**, 229, 153-172.

12) Badia, A.; Carlini, R.; Fernandez, A.; Battaglini, F.; Mikkelsen, S.R.; English, A.M., J. Am. Chem. Soc., **1993**, 115, 7053-7060.

13) Foulds, N.C.; Frew, J.E.; Green, M.J., Biosensors, a Practical Approach, Cass, A.E.G., Ed., **1989**, 119.

14) Ngo, T.T., Electrochemical Sensors in Immunological Analysis, Ngo,T.T, Ed., Plenum Press, New York, **1987**, 103.

2.0 Modification and Characterization of Native GOx

2.1 Introduction

It has been suggested that the carbohydrate moiety of GOx may act as a barrier to electron transfer between the enzyme and an electrode surface[1]. This hypothesis can be tested using the deglycosylated enzyme, and this has been attempted in concurrent work in our laboratory[2]. The carbohydrate moiety could also interfere with derivatization of amino acid residues in GOx. Since derivatization is under investigation here, preliminary studies on deglycosylated GOx (dGOx) were carried out and are described in this chapter.

Glucose oxidase (GOx) from *Aspergillus niger* is a 160 kD dimeric glycoprotein with a carbohydrate content of the high-mannose type which accounts for approximatively 16% of its molecular weight[3]. The carbohydrate moieties are O- and N-glycosidically linked to the protein[4]. N-glycosylation sites can be identified by the consensus sequence Asn-X-Thr/Ser, and from its amino acid sequence [5] it can be seen that there are 8 such sites on GOx[6] (Figure 2.1).

Enzymatic deglycosylation[7] as well as chemical deglycosylation via periodate oxidation[8] have been performed on GOx. Periodate treatment decreased the carbohydrate content by approximately 40% and no significant changes in the catalytic parameters, immunological reactivities, amino acid content, or tertiary or quaternary structure were found in the periodate treated enzyme compared to native GOx[8]. Approximately 95% of the carbohydrate moiety was removed by incubating GOx with deglycosylating enzymes[7]. No major changes were observed in the thermal stability or the circular dichroism spectrum of the deglycosylated enzyme. pH and temperature optima for GOx activity, as well as substrate

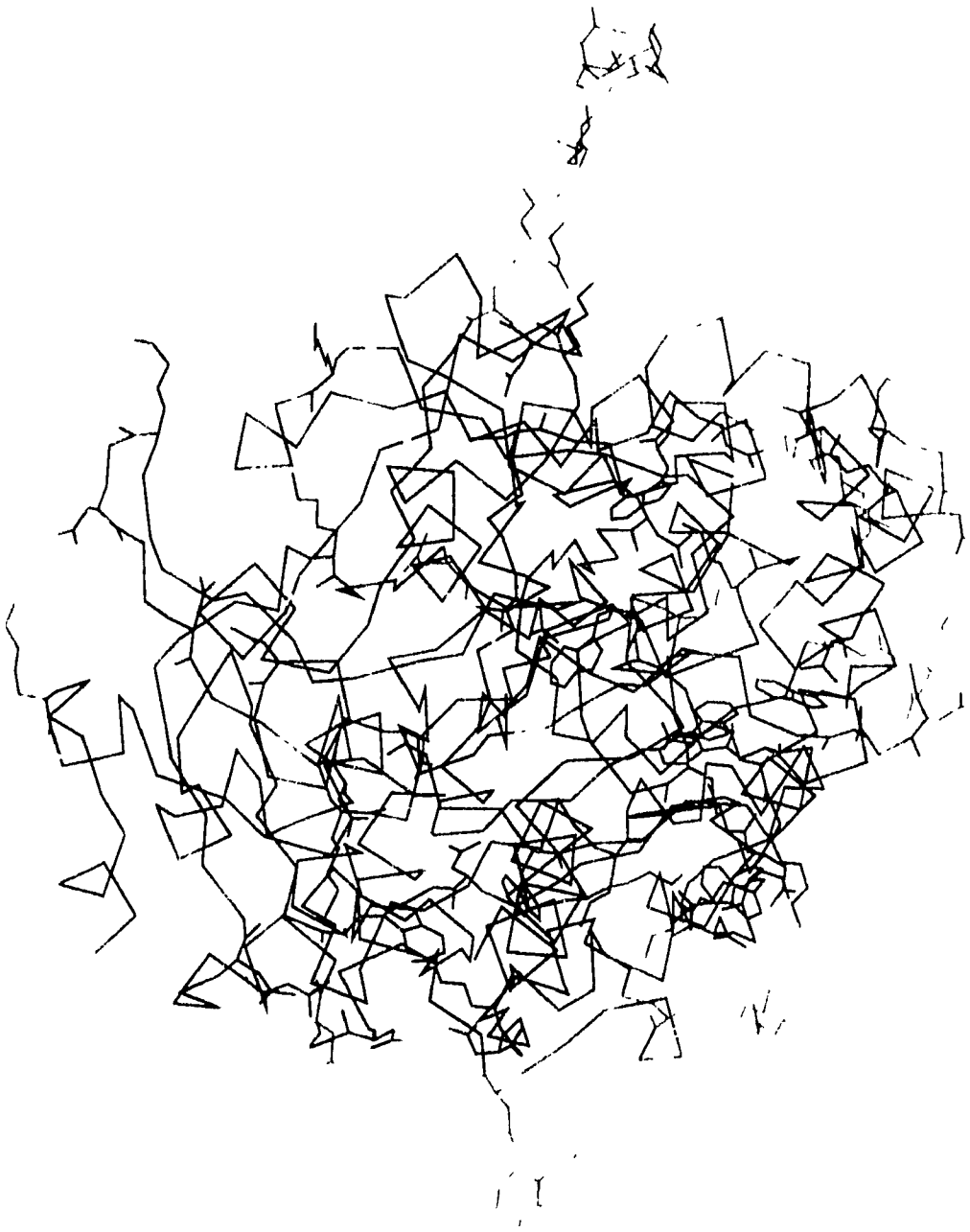

Figure 2.1: N-glycosylation sites in GOx shown on the C_α backbone This figure was generated using the MidasPlus software system from the Computer Graphics Laboratory, University of California San Francisco (UCSF) and the x-ray coordinate of GOx[1]

selectivity were not affected by deglycosylation. Therefore, the carbohydrate moiety of GOx does not seem to contribute detectable effects to the structure, stability and activity of GOx. However, other studies have shown that dGOx precipitates at lower concentrations of trichloroacetic acid and ammonium sulphate than the native enzyme, suggesting that the carbohydrates contribute to the high solubility of GOx in water[8].

The N-glycosylation sites in enzymatically deglycosylated GOx were identified in the x-ray structure from the electron density of the N-acetylglucosamine group attached to Asn residues. These were observable because endoglycosidase H (endo H) cleaves the sugars after the N-acetylglucosamine, and the N-glycosylation sites are shown in Figure 2.1. It was also found that the sugars attached to Asn 89 were not removed since they are involved in subunit interactions. It was postulated from the peptide sequence that Asn 43 was not glycosylated and the crystal structure showed that it is involved in strong hydrogen bonding, which may prevent its glycosylation. O-glycosylation sites cannot be identified from the x-ray structure because the carbohydrates are enzymatically cleaved at the polypeptide chain[3].

Using small molecules such as fluorescein glycine amide (FGA) and 2,4-dinitrobenzoic acid (DNBA), derivatization via EDC-NHS promoted amide bond formation of native GOx was attempted using the schemes shown in Figure 2.2. FGA and DNBA were chosen because the ultimate goal of this work is to develop electrochemical immunoassays using GOx (as discussed in Chapter 3) and antibodies to FGA and DNBA are commercially available.

This chapter outlines the procedures used for the enzymatic deglycosylation of GOx and characterization of dGOx. The latter included electrospray mass spectrometric (ES-MS) studies on GOx and dGOx. Recently a number of reviews have been published on the analysis

Figure 2.2: EDC-NHS promoted amide bond formation between GOx and (a) fluorescein glycine amide (FGA) and (b) 2,4-dinitrobenzoic acid (DNBA).

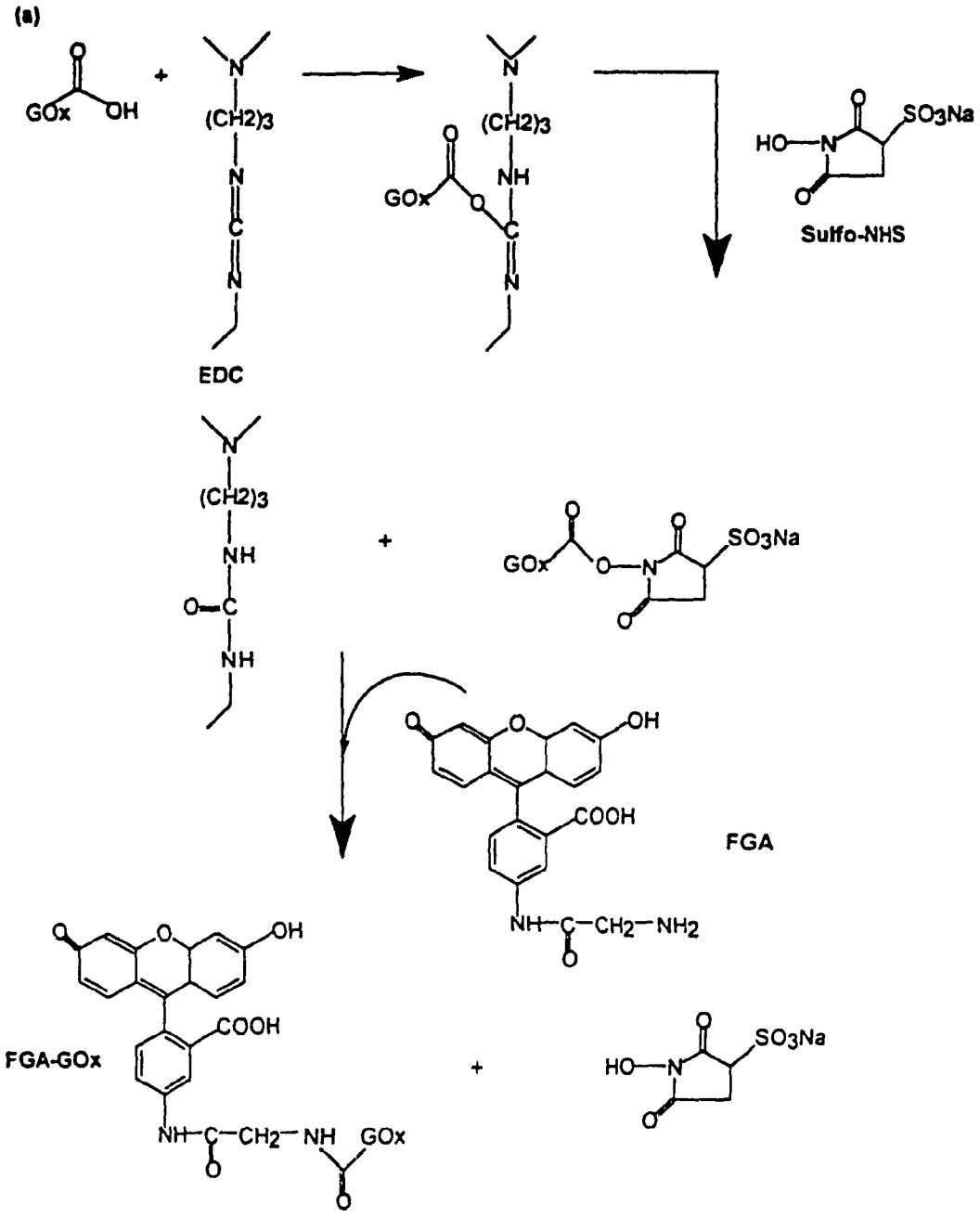
(a)
GOx
OH
(CH2)3
EDC
NH
Sulfo-NHS
SO3Na
HO
FGA
FGA-GOx
COOH

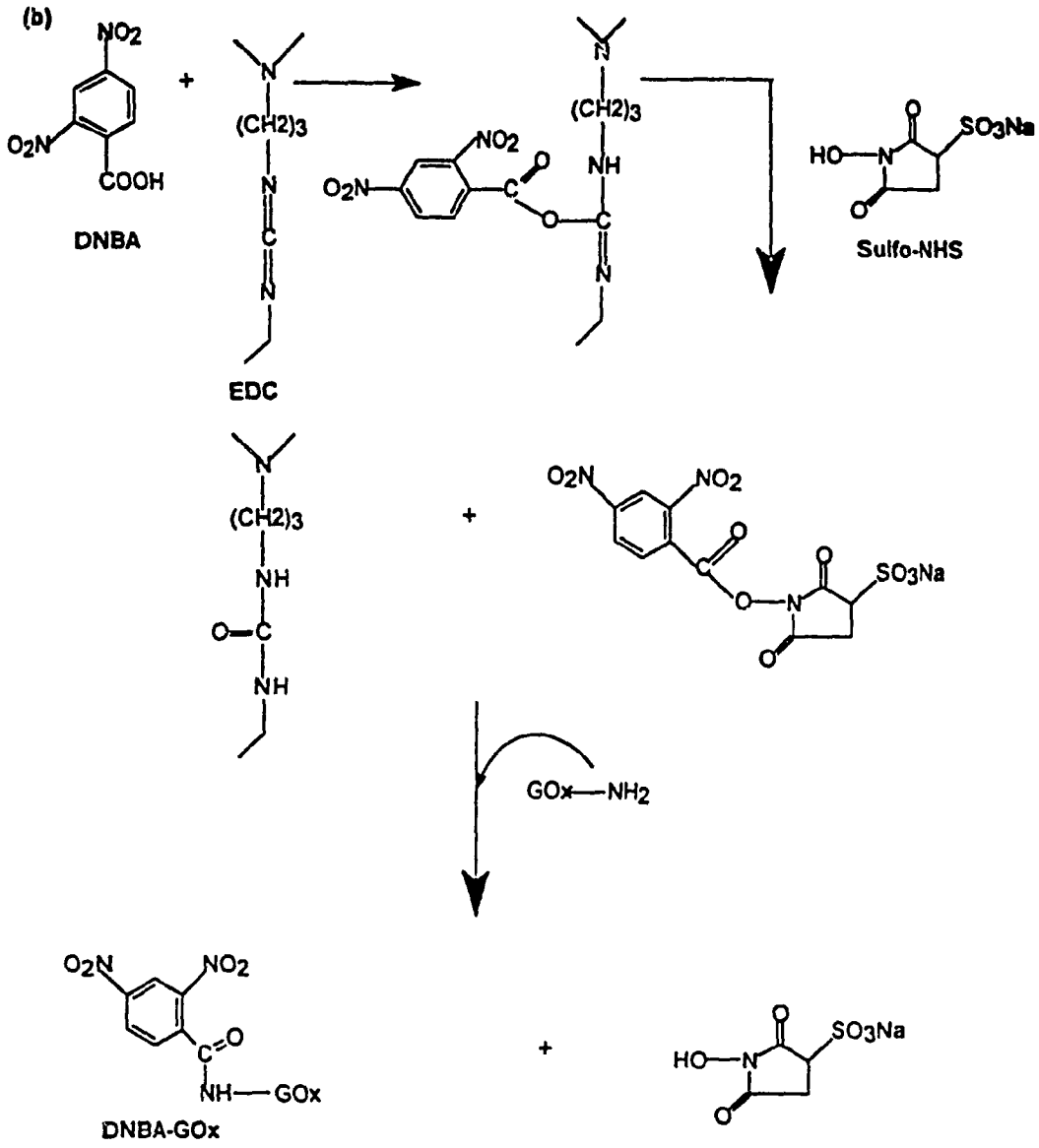
(b)
DNBA
EDC
Sulfo-NHS
GOx—NH2
DNBA-GOx

of biomolecules via ES-MS[9]. However, characterization of glycoproteins by ES-MS is complicated due to the diversity of glycoforms present[10], and the poor electrospray ionization multicharging of the polysaccharide moiety[11]. Results on the characterization of FGA- and DNBA-derivatized GOx will also be presented in this chapter. Unfortunately, time did not permit modification of dGOx with either FGA or DNBA, so no conclusions on the effects of the carbohydrates on modification can be presented.

2.2 Experimental

2.2.1 Materials

Glucose oxidase from *Aspergillus niger* (GOx, E.C. 1.1.3.4, Grade II, lyophilized powder), endoglycosidase H (endo H) and horseradish peroxidase (HRP, E.C. 1.11.1.7) were purchased from Boehringer Mannheim, and α-mannosidase was obtained from Glycosystems. α-D-glucose was obtained from Aldrich and a 1 M stock solution in water was left to mutarotate overnight at 4°C. Fluorescein glycine amide (FGA) was purchased from Molecular Probes. Sulfo-N-hydroxysuccinimide (s-NHS) was obtained from Pierce. o-Dianisidine dihydrochloride, 2,4-dinitrobenzoic acid (DNBA), 4-(2-hydroxyethyl)-1-piperazineethanesulfonic acid (HEPES) and 1-ethyl-3-(3-dimethylaminopropyl)carbodiimide hydrochloride (EDC) were purchased from Sigma. Acrylamide, N,N'-methylenebis(acrylamide) and tetramethylethylenediamine (TEMED) for SDS-PAGE together with a Mini Protean II Electrophoresis Dual Slab Cell were purchased from Bio-Rad. Mono- and dibasic sodium phosphate, mono- and dibasic potassium phosphate, trifluoroacetic acid (TFA) and acetonitrile were purchased from Fisher. Coomassie Brilliant Blue G-250 protein assay dye reagent was purchased from Bio-Rad.

A C_{18} reversed phase HPLC column (0.5 x 27.5 cm) was obtained from Vydac. Sephadex G-25 fine grade molecular exclusion gel, a Mono S HR 10/10 cation-exchange column, and a Phenyl Sepharose (16/10) column were purchased from Pharmacia, who also provided the FPLC system. This was controlled by a LC-500 unit connected to two pumps, a UV-M monitor and a MV-7 motorized valve for sample injection. All FPLC buffers were prepared with distilled, deionized water (specific resistance 18 MΩcm) from a Barnstead Nanopure system, filtered through a 0.45 µm membrane (Gelman Sciences) and degassed by sonication or vacuum prior to use. An ultrafiltration cell and YM 30 filters (MW cutoff 30 000 daltons) were purchased from Amicon. All absorbance measurements were performed on a Hewlett Packard 8451A diode array spectrophotometer or a Beckman DU650 spectrophotometer. The HPLC system used was a HP 1090 with a diode array detector and a HP workstation located at the Biotechnology Research Institute (BRI, National Research Council, Montréal).

2.2.2 Methods

2.2.2.1 Total Protein: The standard Coomassie Blue procedure from Bio-Rad was used to determine total protein concentrations spectrophotometrically at 595 nm. A calibration curve was made with native GOx concentrations ranging from 5 to 25 µg/ml, and the unknown GOx samples were diluted in order that their absorbances fell within the range of the calibration curve.

2.2.2.2 Homogeneous Activity Assay: GOx activity was determined by a coupled assay as follows:

$$\beta\text{-D-glucose} + H_2O + O_2 \xrightarrow{GOx} \text{D-glucono-}\delta\text{-lactone} + H_2O_2 \qquad (2.1)$$

$$2\,H_2O_2 + 2\,DH_2 \xrightarrow{HRP} 4\,H_2O + D_2 \qquad (2.2)$$

The H_2O_2 produced in Reaction 2.1 by the GOx-catalyzed reduction of O_2 by glucose was detected by following the HRP-catalyzed oxidation of a dye, o-dianisidine, in the second step ($\epsilon_{436} = 8.3 \times 10^3\ M^{-1}cm^{-1}$). The assay was carried out in air-saturated 0.1 M potassium phosphate buffer, pH 7.0, and the concentration of reagents in the assay solution were as follows: 2.4×10^{-5} M o-dianisidine, 0.092 M β-D-glucose and 6.5×10^{-3} mg/ml HRP. Depending on the sample, the concentration of GOx in the assay solution varied from 4 to 50 nM, and the total volume in the cuvette was 3.06 ml. The change in absorbance at 436 nm was measured over 3 min. Enzyme activities are always given relative to commercial GOx, which was taken as 100% unless otherwise specified.

2.2.2.3 Purification of Commercial GOx: The commercially-available enzyme was purified by hydrophobic interaction chromatography (HIC) on a Phenyl Sepharose (16/10) FPLC column equilibrated with 1.7 M $(NH_4)_2SO_4$ in 20 mM phosphate buffer, pH 7.5. The sample size loaded was 5 mg in 0.5 ml of starting buffer, and elution was by dilution of the ionic strength with 20 mM phosphate buffer, pH 8.0. The flow rate was 1.0 ml/min, the fraction size was 4.0 ml, and the absorbance was followed at 280 nm.

2.2.2.4 Modification of GOx with FGA: GOx and FGA, 0.25 and 5.7 μmol respectively, were dissolved in 20 ml of 0.1 M phosphate buffer, pH 7.0. 15 ml of this

solution were pipetted into a second flask to which 1.6 mmol of EDC and 76 μmol of s-NHS were added. The remaining 5 ml in the first flask was used as a control, and both flasks were placed at 4°C overnight. The samples were concentrated by ultrafiltration using a YM 30 membrane and gel-filtered on a Sephadex G-25 column (0.8 x 26 cm). The concentration of FGA in the gel-filtered samples was determined spectrophotometrically using the absorbance at 489 nm ($\epsilon_{489} = 6.5 \times 10^4\ M^{-1}cm^{-1}$), and the concentration of GOx was determined by the total protein assay. The average number of FGA bound to GOx was found from the ratio of FGA to GOx.

2.2.2.5 Modification of GOx with DNBA: 188 μmol of 2,4-DNBA were dissolved in 4 ml of 0.15 M NaHEPES, pH 7.4, and stirred for 10 min. 188 μmol of EDC and 281 μmol of s-NHS were added respectively and the solution was left to stir in an ice bath for 30 min. GOx (0.38 μmol) was added and a control solution containing GOx and 2,4-DNBA only was also prepared and both were covered and left at 4°C overnight The samples were concentrated by ultrafiltration and gel-filtered on a Sephadex G-25 column An attempt was made to determine the concentration of nitro groups in the gel-filtered samples by dissolving the samples (3 to 5 mg) in acetone. 20 ml of 11 N HCl were added and the air was removed using a N_2-purge for 5 min. Ferrous ammonium sulphate (1.5 to 2 g) was added, the solution was boiled for 15 min and left to cool. A 10% solution of ammonium thiocyanate (1 ml) was added to develop a red color[23]. The absorbance of the samples was measured at 330 and 460 nm. Free DNBA was used to prepare standard curves in the presence and absence of native GOx.

2.2.2.6 SDS-PAGE of Purified GOx: A 7.5% denaturing gel was prepared by

adding 4.85 ml of distilled water, 2.50 ml of 1.5 M Tris-HCl pH 8.0, 100 µl of 10% w/v SDS and 2.5 ml of acrylamide/bis (from a 30% stock). The solution was degassed for 15 min and 50 µl of fresh ammonium persulfate (10% w/v) and 5 µl of TEMED were added. The solution was immediately poured between the glass plates and saturated n-butanol was added to flatten the surface of the gel. The gel was left to polymerize and then rinsed with water to remove the n-butanol before the addition of a 4% stacking gel, which was prepared as follows: 6.1 ml of distilled water, 2.5 ml of 0.5 M HCl, pH 6.8, 1.3 ml of acrylamide/bis (from a 30% stock) and 100 µl of 10% (w/v) SDS were mixed and the resulting solution was degassed for 15 min; ammonium persulfate (50 µl) and TEMED (10 µl) were added to initiate the polymerization. The stacking gel solution was then poured on top of the running gel, a comb was inserted to form the lanes, and the solution was left to polymerize. After polymerization the comb was removed, the cell was assembled, and the running buffer was poured in the chamber. A sample of GOx was dissolved in the sample buffer, which contains bromophenol blue as a tracking dye, glycerol and 10% SDS, and heated for 10 min. GOx from the bottle and the HIC-purified GOx fractions (2-4 µg per lane) were loaded on the gel. Broad-range molecular weight standards (Bio-Rad) were run along with the GOx samples to give a distribution of bands between 45 - 200 kD. The applied voltage was 50 V until the samples had run through the stacking gel, and then the voltage was increased to 100 V. The gel was stained using a 0.25% Coomassie blue solution and destained using a solution of water, methanol and acetic acid in a ratio of 5:4:1.

2.2.2.9 Deglycosylation of GOx: Following the literature procedure[7], 1 mg of HIC-purified GOx was incubated at 37°C for 24 h with 6 U of α-mannosidase and 20 mU of endo

H in 30 mM potassium phosphate, pH 5.0, in a total volume of 3.0 ml. A control was run by incubating 1 mg of GOx under the same conditions but in the absence of the deglycosylating enzymes. The deglycosylated GOx (dGOx) samples were passed through a 0.8 x 26 cm Sephadex G-25 gel filtration column equilibrated with 30 mM phosphate buffer, pH 5.0. The protein, which appeared in the void volume, was concentrated and applied to a cation-exchange Mono S HR 10/10 FPLC column equilibrated with 20 mM phosphate buffer, pH 4.2. The sample size loaded was 1-2 mg in 0.5 ml of 20 mM phosphate buffer, pH 4.2. dGOx was eluted with a 0-1 M NaCl gradient in 20 mM phosphate buffer, pH 4.2. The flow rate was 1.0 ml/min, the fraction size was 4 ml and the absorbance was followed at 280 nm. SDS-PAGE of dGOx was carried out as described in Section 2.2.2.6. dGOx (1-3 μg) was loaded on the gel, as well as the native GOx control. A dGOx sample (0.9 mg/ml) obtained from the cation-exchange column was injected (210 μl) onto a 0.5 x 27.5 cm C_{18} reverse phase column at room temperature that had been equilibrated with 0.1% TFA in water (pH 2.85). The samples were eluted with a 10 to 70% acetonitrile gradient in 0 1% TFA. The absorbance of the eluate was followed at 210 nm, 280 nm and 465 nm. The flow rate was 1.0 ml/min and the fraction size was 1.0 ml. HPLC purification of dGOx was carried out to remove the salts from the samples before ES-MS because salts interfere with the MS measurements.

2.2.2.10 ES-MS of dGOx: ES-MS was carried out at BRI by George Tsaprailis and Bernard Gibbs. Mass spectra were obtained using the positive ion mode of a triple stage mass spectrometer (model API-111, Sciex, Toronto, Canada). Samples (0 1 - 1.0 μg/ μl) of native GOx and dGOx dissolved in 10% acetic acid, were infused through a stainless steel capillary

(ID = 1×10^{-4} m), and a stream of air was introduced to assist in the formation of submicron droplets. These were evaporated at the interface by N_2 gas producing highly charged ions which were detected by the mass analyzer.

2.2.2.11 Amino Acid Analysis: These analyses were also carried out by Bernard Gibbs at BRI. Samples were placed in tubes which had been previously muffled at 450°C overnight. The tubes were placed in a Waters reaction vial and the samples were dried in a Waters Pico-Tag workstation. 200 µl of 6 N constant boiling HCl containing 1% phenol was added to the vials which were alternatively purged with nitrogen and evacuated. The hydrolysed residue was dissolved in sodium citrate at pH 3 and applied to a Beckman System 7300 High Performance Analyzer according to the general procedure of Spackman et al[12].

2.3 Results

2.3.1 Purification of Commercial GOx: Different buffers and gradients were tested in order to determine the best conditions for purification of commercial GOx by HIC Figure 2.3(a) shows the best HIC chromatogram obtained, and the conditions are given in Section 2 2.2 3. Peaks 1 and 2 were eluted at 18 and 27 ml, respectively. It was observed that if GOx was gel-filtered before loading it onto the HIC FPLC column, peak 2 was drastically reduced as can be seen from Figure 2 3(b). If free flavin adenine dinucleotide (FAD) was added to GOx after the gel filtration and the mixture reloaded onto the HIC column, a narrow band (Figure 2.3(c)) replaced the broad band which was initially observed at 27 ml in Figure 2 3(b). The concentration of protein in the gel-filtered GOx and the two peaks from the HIC column in Figure 2.3(a) were determined using the Bio-Rad total protein assay. (A typical standard curve obtained for total protein assay is shown in Figure 2.4). Both peaks 1 and 2

Figure 2.3: FPLC hydrophobic interaction chromatography (HIC) of GOx on a 1.6 x 10 cm Phenyl Sepharose column equilibrated with 1.7 M $(NH_4)_2SO_4$ in 20 mM phosphate buffer, pH 7.5, and elution was by dilution of ionic strength with 20 mM phosphate buffer, pH 8.0. (a) 5 mg of commercial GOx, (b) 5 mg of GOx that has been gel-filtered on a Sephadex G-25 column (0.8 x 26 cm) and (c) 5 mg of gel-filtered GOx spiked with free FAD. The flow rate was 1.0 ml/min, the fraction size was 4 ml and the absorbance was followed at 280 nm. The solid line represents the percentage of 20 mM phosphate buffer (pH 8.0) in the eluent

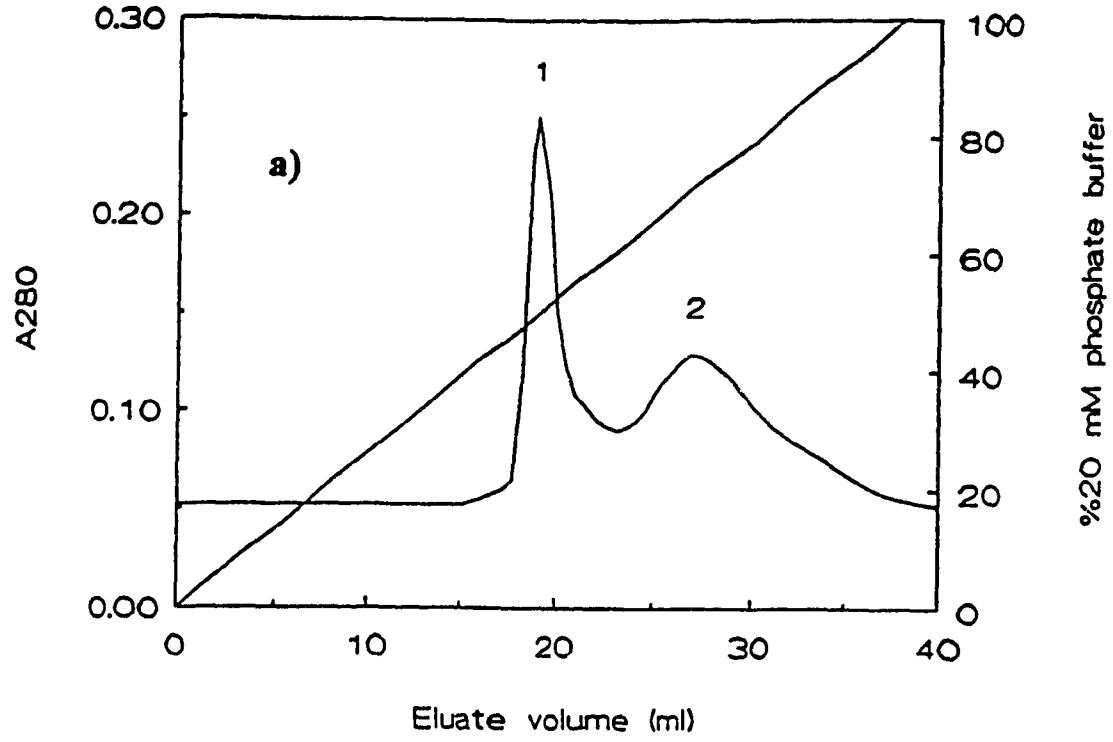
a)
1
2
A280
0.30
0.20
0.10
0.00
0
10
20
30
40
100
80
60
40
20
0
%20 mM phosphate buffer
Eluate volume (ml)

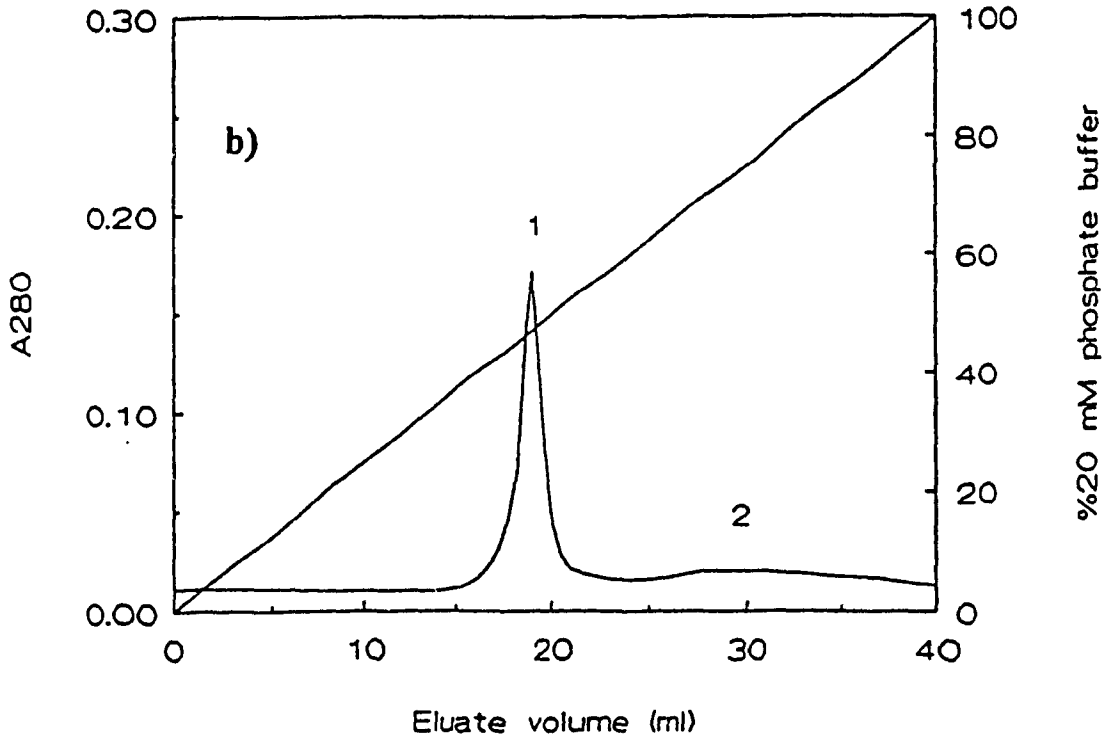
b)
1
2
A280
0.30
0.20
0.10
0.00
0
10
20
30
40
100
80
60
40
20
0
%20 mM phosphate buffer
Eluate volume (ml)

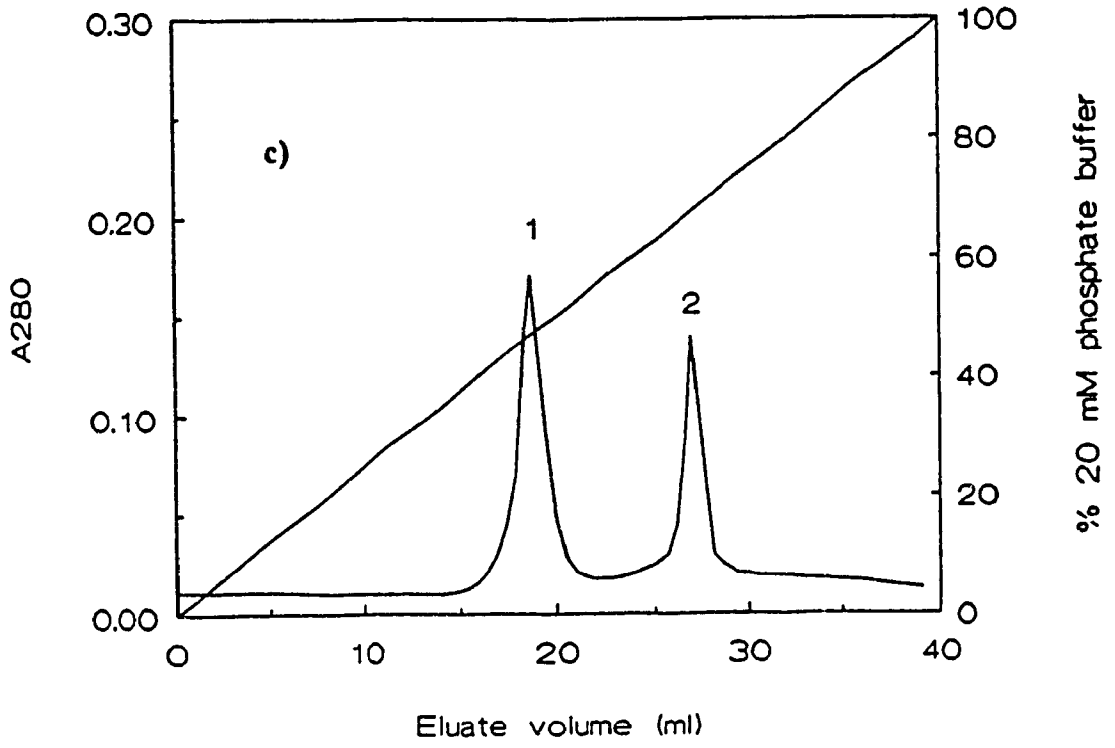
0.30
0.20
0.10
0.00
A280
c)
1
2
0
10
20
30
40
Eluate volume (ml)
100
80
60
40
20
0
% 20 mM phosphate buffer

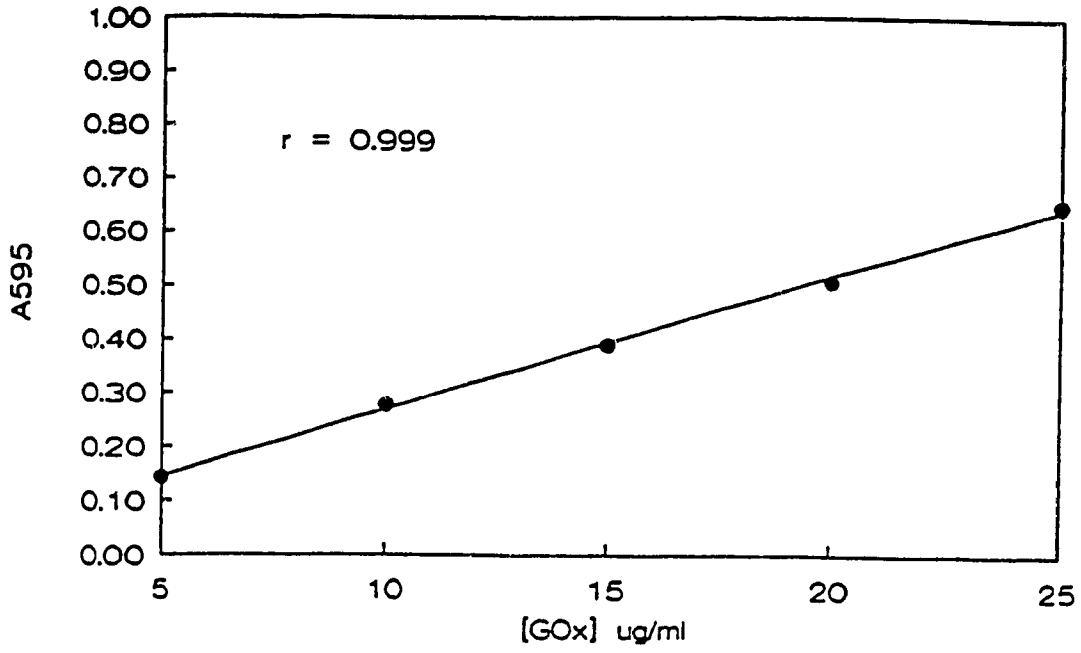

Figure 2.4: Bio-Rad total protein assay. The calibration curve was prepared using native GOx solutions in 0.01 M phosphate buffer, pH 7.0, having concentrations ranging from 5 to 25 μg/μl. The absorbance of these solutions was measured at 595 nm.

were found to contain protein, hence free FAD is not the only component in peak 2. The activities of the GOx that had been subjected to gel-filtration only and of GOx that had been subjected to both gel filtration and HIC (Figure 2.3(b)) were determined, and the results are given in Table 2.1. Both peak 1 and the small peak 2 from the HIC column exhibit GOx activity, and peak 1 was found to be more active than commercial GOx from the bottle. These results suggest that two forms of GOx are present in the commercial sample giving rise to the two peaks observed in Figure 2.3(a) and (b). However, the significant reduction in peak 2 following gel filtration on G-25 suggests that the species contained in this peak can be converted to that in peak 1 by the removal of some low molecular weight compound(s). Since free FAD is observed on the top of the G-25 column it is speculated that nonspecific interactions between FAD and GOx in the commercial sample give rise to peak 2. The UV-Vis spectra of peak 1 and 2 from Figure 2.3(b) are compared in Figure 2.5 to GOx from the bottle. All three samples exhibit the expected GOx absorption maxima at 382 and 452 nm[13].

Table 2.1 : Activity of GOx after Each Purification Step[a]

Sample	% Relative Activity
Commercial GOx	100
After gel filtration	102
Peak 1 from HIC	111
Peak 2 from HIC	102

[a] Activity measured as described in Section 2.2.2.2

2.3.2 SDS-PAGE of HIC Purified GOx: Peaks 1 and 2 collected from the HIC

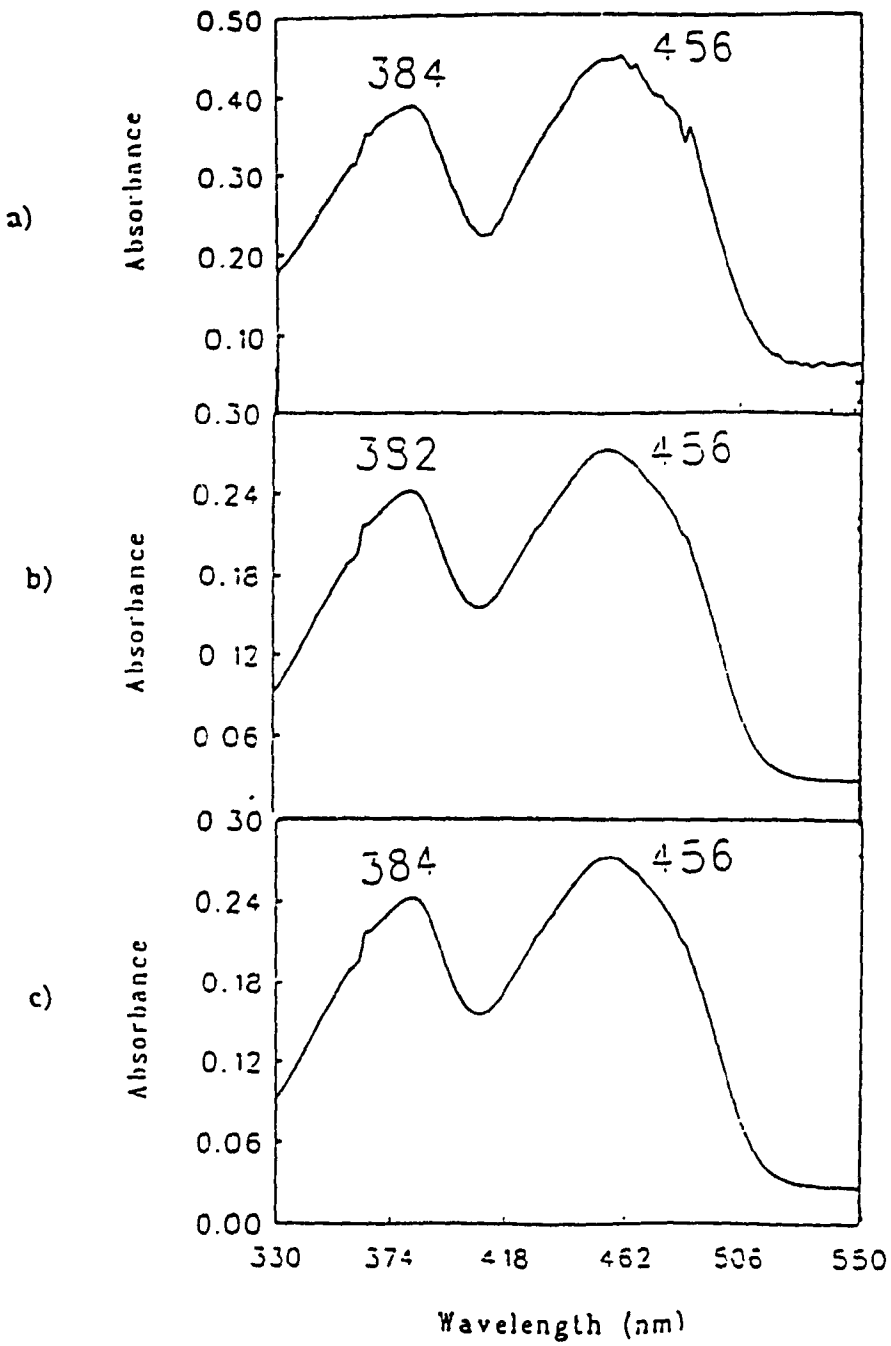

Figure 2.5: UV-Vis spectra of (a) native GOx (b) peak 1 from HIC and (c) peak 2 from HIC (Figure 2.3 (b)). All samples in 0.1 M phosphate buffer, pH 7.0, and cuvette pathlength of 1 cm.

column (Figure 2.3(b)) were analyzed by SDS-PAGE on a 7.5% gel. The same concentration of sample was loaded in each well, and it was confirmed from the gel that both peaks 1 and 2 contained GOx since the distance migrated by both these samples corresponds to that of GOx from the bottle. It is noteworthy that the bands in the SDS gel containing HIC-purified GOx were sharper than the corresponding band for the unpurified enzyme.

2.3.3 Characterization of Modified GOx: From the FGA absorption at 489 nm and total protein analysis (Section 2.2.2.1), GOx was found to be modified with an average of 5 molecules of FGA. Thus, the FGA-modified enzyme will be designated as $(FGA)_5$-GOx

The calibration curves prepared for free DNBA in the presence and absence of native GOx are shown in Figure 2.6. A comparison of the two curves shows that the addition of GOx did not significantly change the curve, except that the absorbance values are a little it higher. A sample of GOx that was subjected to the DNBA modification procedure (Section 2.2.2.5) was treated with the ferrous ammonium sulphate and ammonium thiocyanate reagents but the absorbance at 330 nm was the same as a control containing native GOx. Equations 2.3-2.4 give the reactions involved in the determination of the nitro groups by the iron and thiocyanate reagents, where DNBA is 2,4-diaminobenzoic acid

$$DNBA + 12\,Fe^{2+} + 12\,H^{+} \longrightarrow DABA + 4\,H_2O + 12\,Fe^{3+} \quad (2.3)$$

$$Fe^{3+} + 6\,SCN^{-} \longrightarrow \underset{\text{red colour}}{[Fe(SCN)_6]^{3-}} \quad (2.4)$$

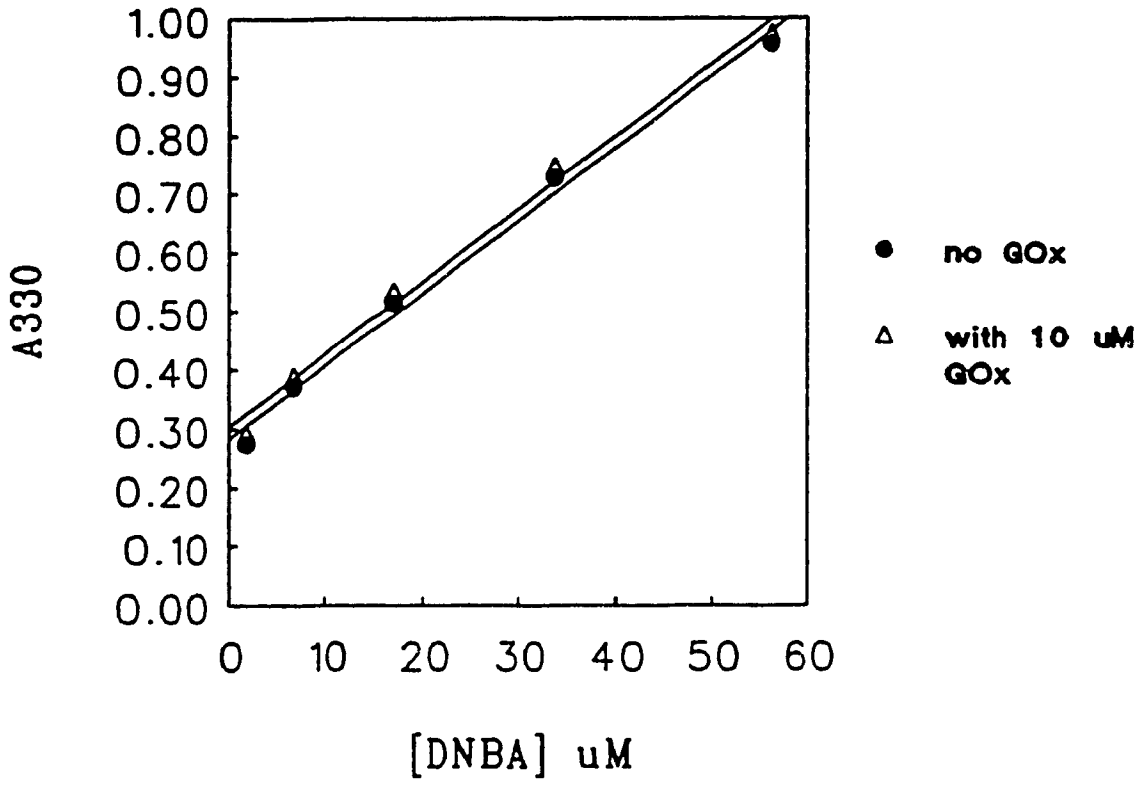

Figure 2.6: Standard curve of the absorbance at 330 nm vs concentration of free DNBA in the presence and absence of GOx. The experimental procedure are described in Section 2.2.2.5.

Since 10 μM GOx was used for this determination of DNBA, enzyme modified with 1:1 DNBA should exhibit an absorbance of 0.45 at 330 nm, which is above that of the unmodified enzyme (Figure 2.6). Therefore, the results suggest that either the enzyme was not modified with DNBA or that the nitro groups of GOx-bound DNBA are not accessible or reactive with the reagents. The latter explanation is preferred since in this laboratory it has been routinely demonstrated that at least 12 Lys in GOx are readily modified using the reagents in Figure 2.2(b). Also evidence is presented in Chapter 3 that GOx has been modified with DNBA. Hence, in this thesis the DNBA-modified GOx is designated as $(DNBA)_x$-GOx. The homogeneous activity of both $(FGA)_5$-GOx and $(DNBA)_x$-GOx were determined and are found in Table 2.3.

Table 2.2: Activity of modified-GOx[a]

Samples	Native	GOx Exposed to Reagents	Modified GOx
$(FGA)_5$-GOx	100	84	47
$(DNBA)_x$-GOx	100	89	83

[a] Activity measured as described in Section 2.2.2.2

In both cases there is initial activity loss upon exposure to the modification reagents alone. A more significant loss is observed for $(FGA)_5$-GOx than for $(DNBA)_x$-GOx, therefore, carboxylic acid groups involved in FAD binding to GOx could have been modified, since FAD loss for this sample was also observed.

2.3.4 Purification of dGOx: After G-25 gel filtration, where dGOx was eluted in

the void volume because of its high molecular weight, the sample was loaded on a Mono-S cation-exchange column. Since the reported pI for dGOx is 4.1- 4.2[7], it did not bind to the cation-exchange column under the conditions used (20 mM phosphate buffer, pH 4.2) and was eluted in the void volume (Figure 2.7). However this chromatographic step served to remove the cleaved carbohydrate and the deglycosylating enzymes since these were eluted at higher salt concentrations. The activity of dGOx and its control were determined and these are found in Table 2.2.

Table 2.3: Activity of GOx after Deglycosylation[a]

Sample	% Relative Activity
Commercial GOx	100
Control GOx[b]	88
dGOx	87

[a] Activity measured as described in Section 2.2.2.2

[b] Control GOx was incubated and purified using the same conditions as for dGOx, but without the deglycosylating enzymes

2.3.6 SDS-PAGE of dGOx: A plot of distance migrated vs the log MW was constructed for the standards (Figure 2.9). From this plot the MW of dGOx was estimated from its migration distance. An examination of the SDS gel reproduced in Figure 2.8 shows that native GOx does not migrate as far as the samples that had been subjected to deglycosylation. This implies that dGOx has lower MW than the native enzyme, and the MWs estimated by SDS-PAGE are summarized in Table 2.3. The two GOx samples that

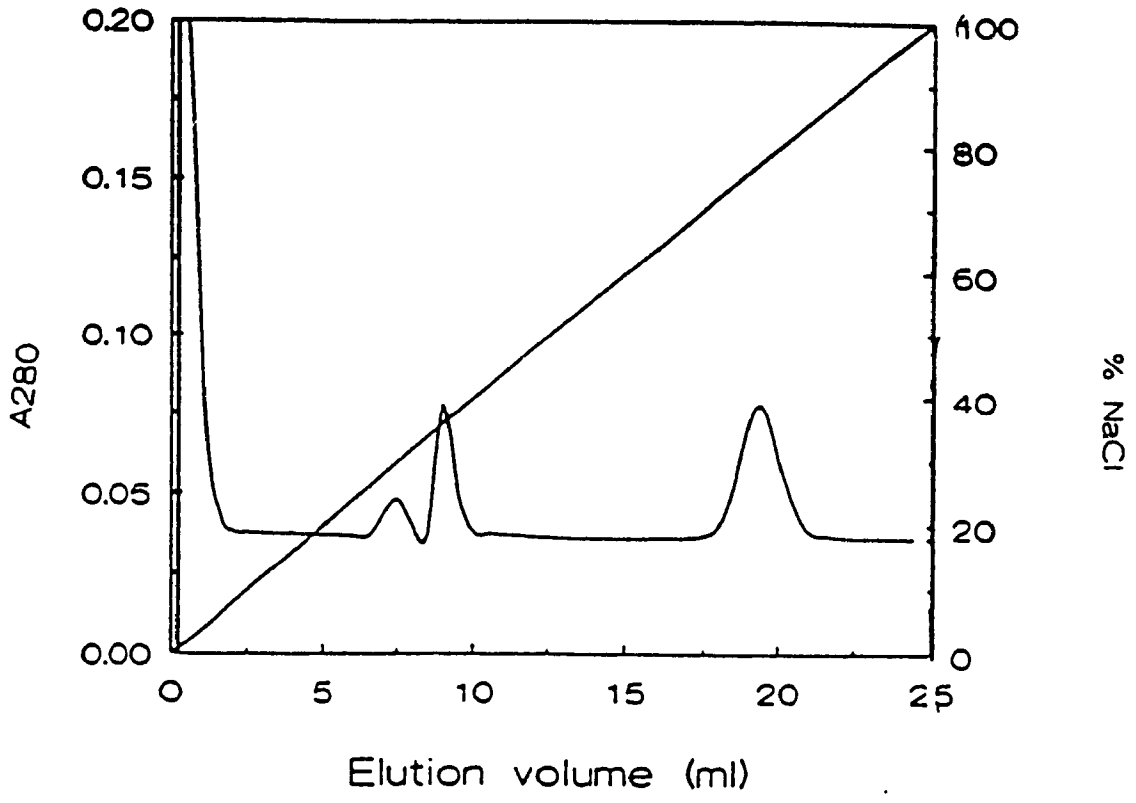

Figure 2.7: FPLC cation-exchange chromatography of 1 mg dGOx on a Mono S (HR. 10/10) column with 20 mM phosphate buffer, pH 4.2 Elution was carried out with a 0-1 M NaCl gradient in 20 mM phosphate buffer, pH 4.2. The flow rate was 1.0 ml/min, the fraction size was 4 ml and the absorbance of the eluate was monitored at 280 nm

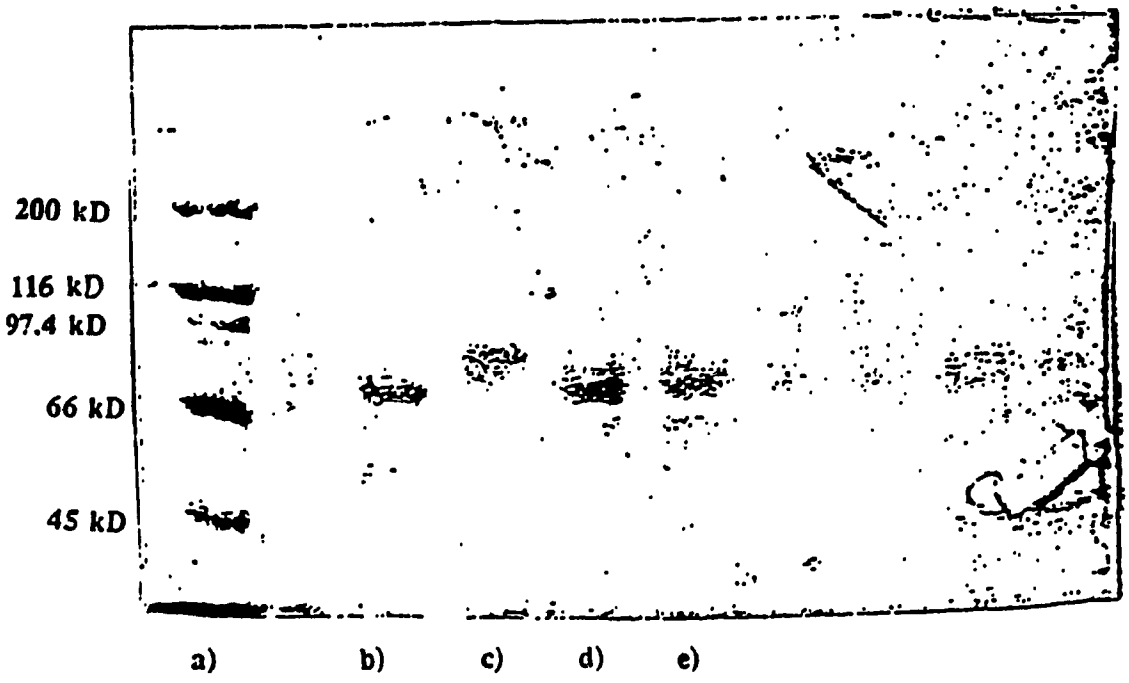

Figure 2.8: SDS-PAGE of native and dGOx

Key: Lane (a) molecular weight standards; (b) dGOx sample from A. Fernandez[2]; (c) native GOx; (d) dGOx (A) and (e) dGOx (B)

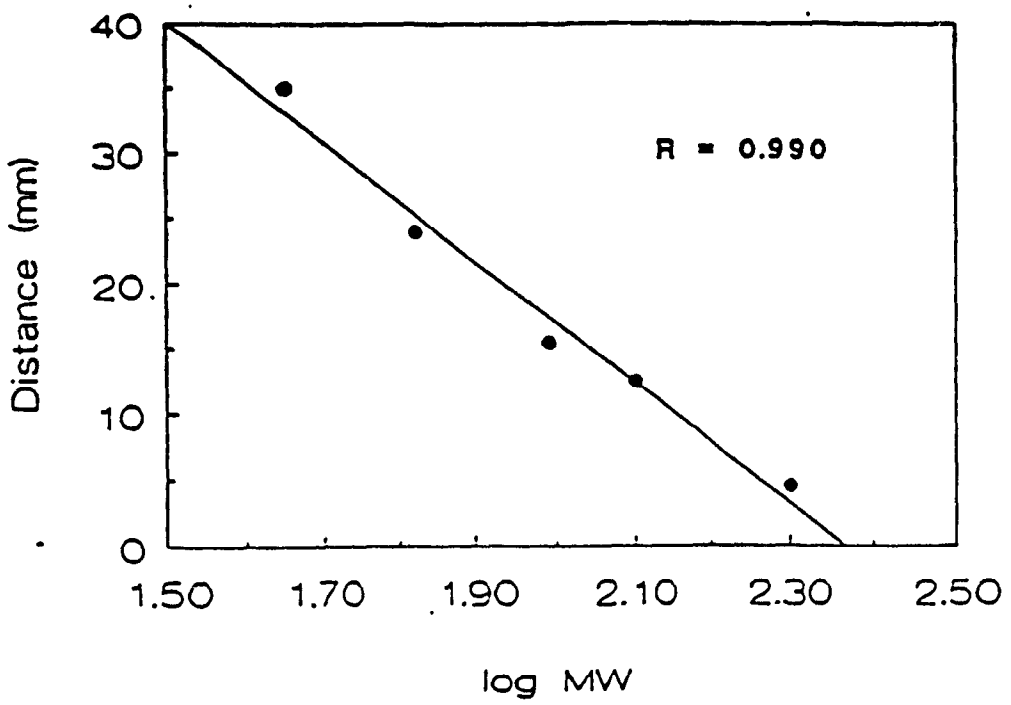

Figure 2.9: Distance migrated vs log MW for the MW standards used in SDS-PAGE SDS-PAGE was carried out as described in Section 2.2.2.6.

were deglycosylated for this work in separate experiments are labelled dGOx (A) and dGOx (B) in Table 2.3 and throughout the thesis.

Table 2.4: Estimate of % Mass Loss of GOx by SDS-PAGE[a]

Sample	Distance migrated (mm)	Molecular weight (kD)[b]	% Mass Loss
control GOx	19 5	88.3	0
dGOx (A)	20.5	84.0	5.2
dGOx (B)	21 0	81.9	7.2

[a] A 7.5% denaturing gel was prepared as described in Section 2.2.2.6

[b] Obtained from the linear regression line of distance migrated vs log MW (Figure 2.9)

The MW obtained for the control is higher than the literature value of 80 kD reported for the GOx monomer[7]. Assuming that the % mass loss is due to deglycosylation the SDS results indicate that GOx is 5-7% glycosylated. This is considerably less than the reported glycosylation value of ~ 15%[7]. However, MW determinations by SDS-PAGE are only accurate to ±5-10%. Also, carbohydrates interfere with SDS binding to proteins which can result in lower charging and altered migration of glycoproteins in SDS gels[15].

2.3.7 ES-MS of dGOx: Figure 2.10 presents the HPLC chromatograms obtained for sample (A) of dGOx (dGOx (A)) at 210 nm, 280 nm and 465 nm, respectively. The peptide backbone is monitored at 210 nm and the aromatic residues (Trp, Tyr, Phe) at 280 nm, whereas at 465 nm FAD is monitored

Figure 2.10: HPLC chromatograms (Vydac C_{18}, reversed-phase column, gradient 0 to 70% acetonitrile in 15 min) of 210 µl of dGOx at a) 210 nm, b) 280 nm and c) 465 nm

a)

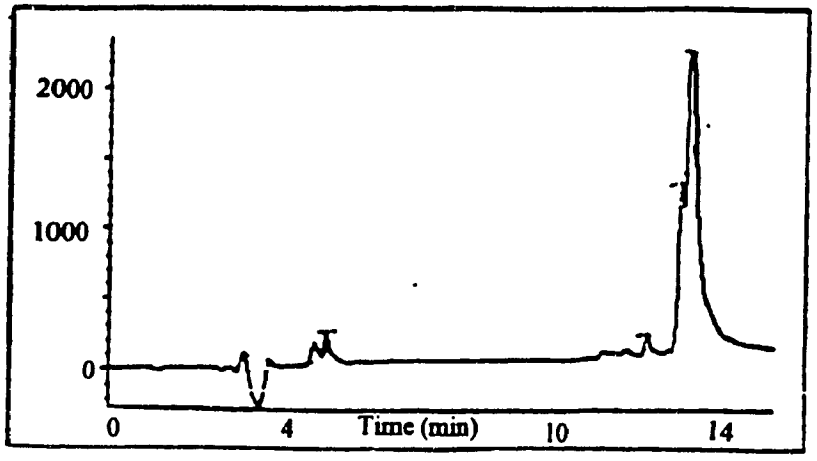
2000
1000
0
0
4
Time (min)
10
14

b)

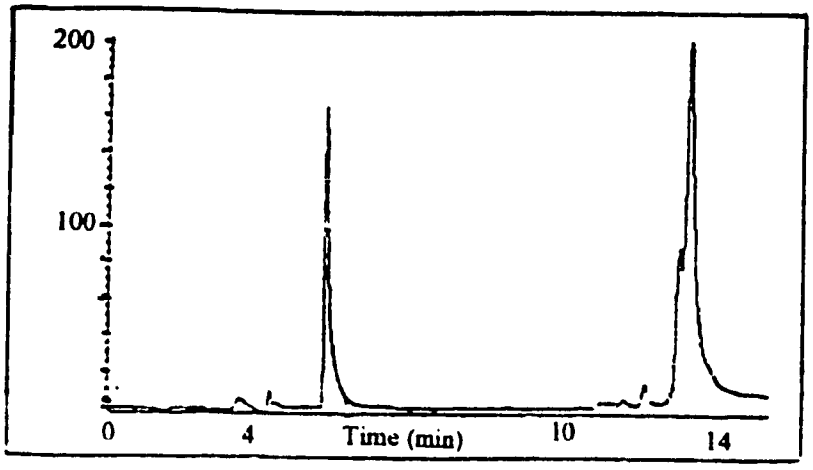
200
100
0
4
Time (min)
10
14

c)

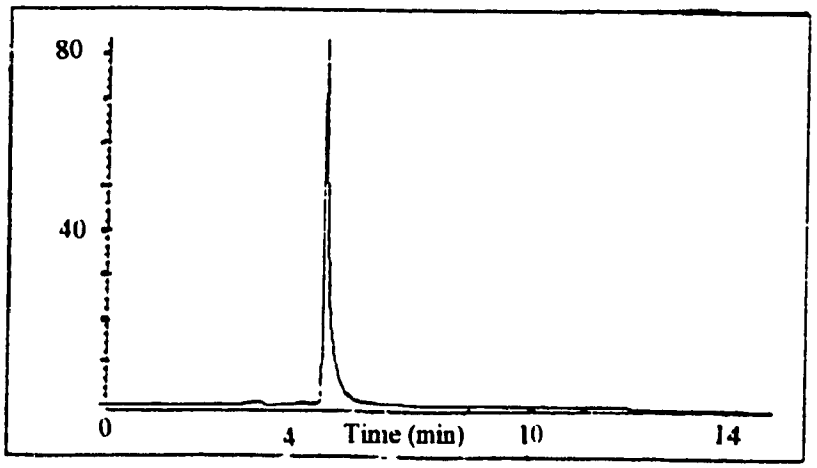
80
40
0
4
Time (min)
10
14

The peak that elutes at 5 min contains free FAD since it absorbs weakly at 210 nm but strongly at 465 nm. The peak at ~ 13.5 min is dGOx, and this was confirmed by amino acid analysis. As can be seen from Figure 2.10 the dGOx peak has a shoulder at ~ 13 min which could be partially deglycosylated forms of GOx.

The mass spectra of native GOx, dGOx (A) and dGOx (B) are shown in Figures 2.11 and 2.12. The MWs found for native GOx as well as for two samples of dGOx are found in Table 2.5.

Table 2.5: Estimate of % Mass Loss of GOx by ES-MS[a]

Sample	Molecular weight	% Mass Loss[b]
native	80 791	0
dGOx (A)	68 149	15.8
dGOx (B)	67 340	16.8

[a] ES-MS was carried out as described in Section 2.2.2.10

[b] Based on decrease in MW

The MW found for the native enzyme is in close agreement with the reported molecular weight of 80 kD per monomer[7]. Monomeric forms of GOx were expected to be observed in ES-MS since the protein denatures under the conditions used here (10% acetic acid). Using the known sequence of GOx[5] and MacProMass software (Version 1.04, Sciex), the MW of the polypeptide moiety of GOx was determined to be 63 246 D; thus, the percent glycosylation by weight of GOx is estimated to be 22% from the MW of 80 791 D determined

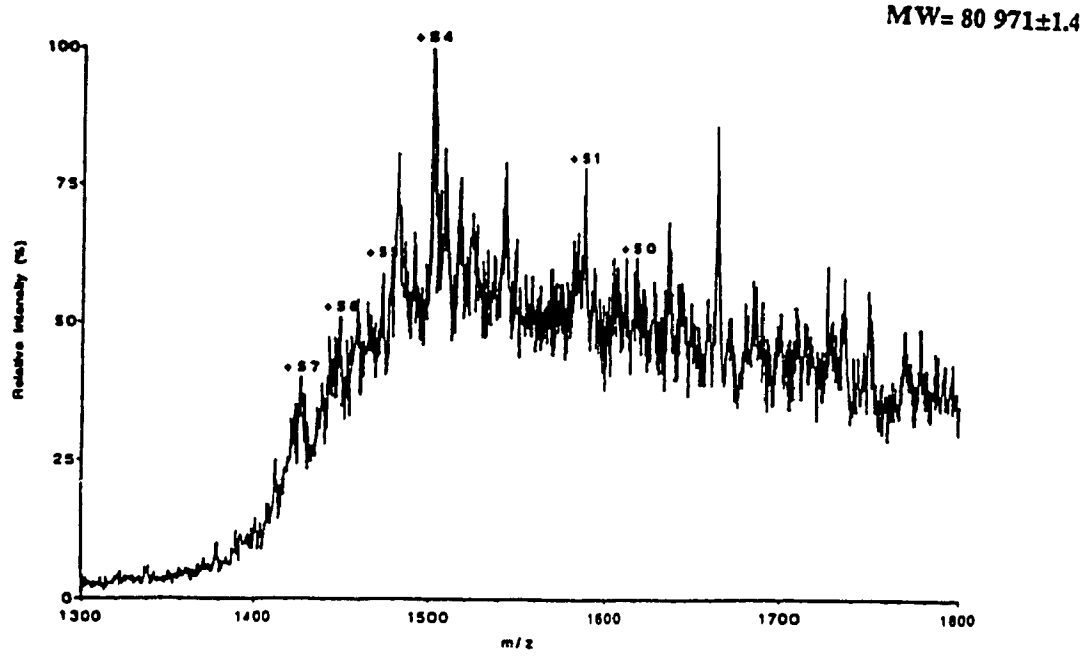

Figure 2.11 ES-MS spectrum of native GOx (1.0 μg/μl) in 10% acetic acid

Figure 2.12: ES-MS mass spectra (1.0 μg/μl) for (a) sample A and (b) sample B of deglycosylated GOx

a)

MW= 68 149± 1.1

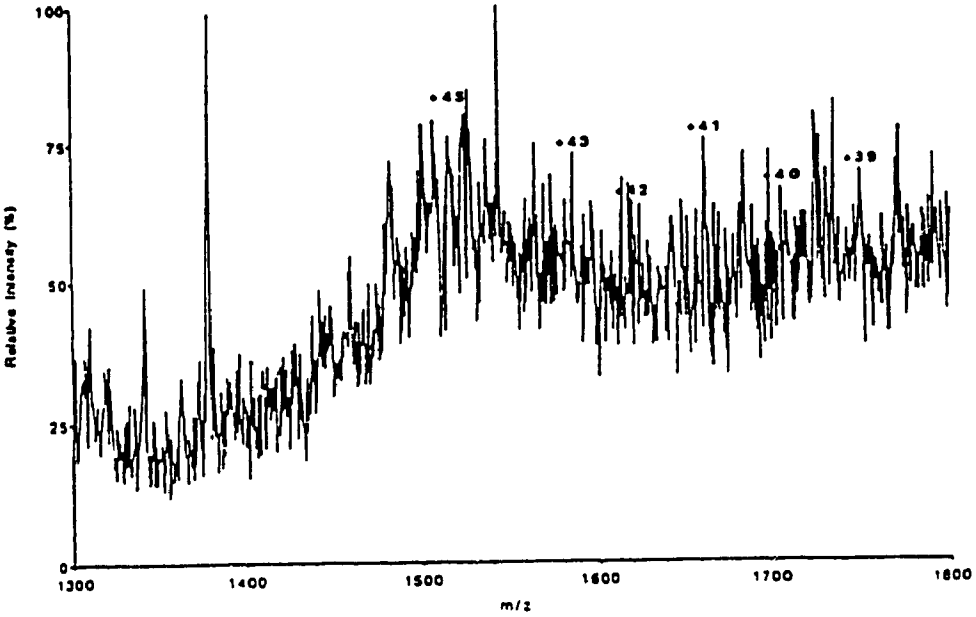

b)

MW= 67 340±1.8

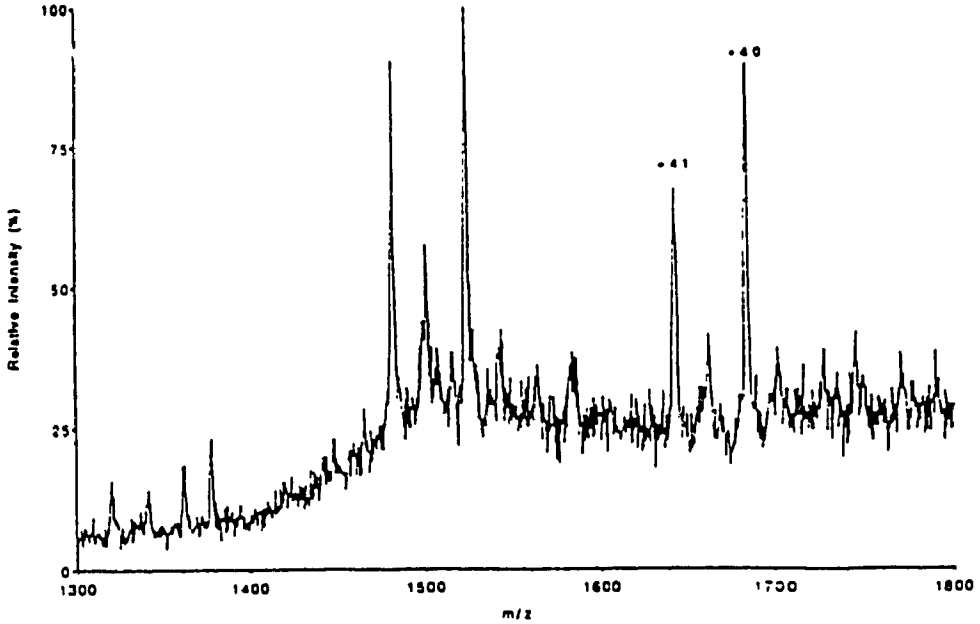

by ES-MS for the holoenzyme. The results obtained by ES-MS for the two samples of dGOx are consistent with the SDS-PAGE results in that the GOx monomer exhibits a lower MW following the deglycosylation procedure. However, the mass loss for dGOx obtained by ES-MS (~16%) is significantly higher than that obtained by SDS-PAGE (~6%). Possible reasons for this discrepancy are given below.

2.4 Discussion

Purification of commercial GOx was carried out using hydrophobic interaction chromatography (HIC) following a literature procedure[7]. Two peaks were observed in the HIC chromatogram, but when GOx was first purified by gel filtration (Sephadex G-25), the second peak was significantly reduced in size (Figure 2 3). Since the sample in this second peak (peak 2) appears to be converted to the same species found in peak 1 following gel filtration, it was assumed above that the G-25 column removed a small MW compound from GOx which altered its interaction with the HIC column. Given that commercial GOx from the bottle was found to contain free FAD, it was speculated that peak 2 contained GOx with nonspecifically bound FAD which altered its interaction with the Phenyl Sepharose gel

In the modification of GOx with FGA the carboxylic acid groups (Glu and Asp) of the protein were targeted, whereas with DNBA the free amino groups (Lys) were the target. GOx contains 15 Lys and 66 carboxylate residues per monomer, and it has been demonstrated that carbodiimides are effective in promoting amide bond formation between these residues and small molecules[16,17]. However, despite their large abundance activation of the carboxylic acid residues on GOx is less facile than activation of the Lys residues Work carried out in this laboratory on the modification of carboxylic acid groups with daunomycin and dopamine

yielded modifier to GOx ratios of 2.5 and 4 for daunomycin and dopamine, respectively[16]. In contrast, targeting Lys residues of GOx with ferrocene derivatives, such as ferrocenecarboxylic acid (FCA), resulted in modifier to GOx ratio of 12. Thus, different ratios of EDC and NHS were used here depending on whether Lys or carboxylate residues were being targeted. For FGA modification, GOx was preincubated for 30 min with a large excess of EDC to promote activation of its carboxylic acid residues and this was followed by addition of NHS and FGA. For DNBA modification, no preincubation was carried out but the molar ratio of NHS used 3.5-fold higher than that used in FGA modification, to generate a high concentration of the DNBA-NHS ester, which is the actual GOx modifier. These results obtained for FGA modification ($(FGA)_5$-GOx) are comparable to the dopamine and daunomycin results obtained previously[18]. The iron-thiocyanate procedure (Section 2.2.2.5) used to determine the ratio of DNBA to GOx yielded inconclusive results. Since all previous work in our laboratory has shown the successful covalent modification of at least 12 Lys residues on GOx, it is very likely that GOx was in fact modified with DNBA. Evidence for DNBA modification is presented in Chapter 3.

Both the SDS-PAGE and ES-MS results reveal partial enzymatic deglycosylation of GOx. However, the extent of deglycosylation indicated by the two techniques is very different. The SDS-PAGE results in Table 2.3 indicate ~6% mass loss upon deglycosylation, whereas the ES-MS results in Table 2.4 indicate a mass loss of ~16%. Both these techniques are not ideal for accurate mass determinations of glycoproteins. Protein MW determination by SDS-PAGE is accurate to ± 5-10%, but the accuracy can be considerably lower for glycoproteins since carbohydrates interfere with SDS binding to polypeptides[14]. MW

determination by ES-MS is accurate to 0.01% for many proteins but the heterogeneity present in a high number of glycoproteins gives rise to mass spectra of poor quality. Such is observed in Figure 2.11 for native GOx, where the "grass-like" appearance of the spectrum reflects the large heterogeneity of the enzyme. Although the labelled peaks in Figure 2.11 correspond to the most abundant glycoform of GOx, it is apparent from the spectrum that may other glycoforms are present in the sample. The hill-shaped background observed in the mass spectrum of native GOx has been observed for other glycoproteins and is not clear what gives rise to this feature[11].

Unfortunately, the mass spectrum obtained for the dGOx (A) sample is of poor quality since high signal-to-noise is observed in regions of the spectrum (e.g. m/z 1300-1400), where any signal from the protein is expected to be negligible. Nonetheless, the most abundant glycoform in dGOx (A) is estimated to have a MW of 68 149 D. This value is very similar to that estimated (67 340 D) for dGOx (B), which gave rise to a mass spectrum of much better quality. In fact, the reduction in the intensity of the "grass" in this spectrum is consistent with considerable deglycosylation of GOx. Analysis of the other two major peaks in the mass spectrum of dGOx (B) yielded a MW of 54 776 D. Using MacProMass software it was determined that cleavage at Tyr506 would result in a GOx fragment with a MW 54 825 D. Traces of proteolytic enzymes, such as trypsin, chymotrypsin and subtilisin, are often found in commercial endo H[17]. Chymotrypsin cleaves at aromatic residues, and since molecular graphics showed that Tyr506 is surface exposed, cleavage at this residue is a definite possibility. A second weak band may be present in the SDS gel for dGOx (B) (Figure 2.8) corresponding to the GOx fragment observed by ES-MS It is also possible that

fragmentation of dGOx (B) occurred during the MS analysis.

By ES-MS, GOx is calculated to be 22% glycosylated. The MWs obtained for native GOx and the dGOx samples from the mass spectra indicate ~16% mass loss due to deglycosylation. If GOx is significantly deglycosylated, then much better agreement between the MWs determined for dGOx by ES-MS and SDS-PAGE is expected. However, the MWs obtained for native GOx using the two techniques differ by only 9% whereas the MWs for the dGOx samples differ by ~23%, which is considerably larger than the error (± 5-10%) in MW determination by SDS-PAGE. Further work is clearly needed to resolve the discrepancy in the results for the dGOx samples.

As reported in the literature, the activity of the dGOx is the same as its native GOx control, which is only 13% less active than GOx from the bottle. Thus, although dGOx may exhibit properties that would make it useful in biosensor development, the high cost of the deglycosylating enzymes and the large amounts required to deglycosylate even mg quantities of GOx, would make the use of dGOx in biosensor development prohibitively expensive.

2.5 References

1) Degani, Y.; Heller, A.J., J. Am. Chem. Soc., **1988**, 110, 2613-2620.

2) Fernandez, A. "Mediated and Direct Electrochemical Studies on Glucose Oxidase", MSc. Thesis, Concordia University, **1994.**

3) Hecht, H.; Kalisz, H.M ; Hendle, J.; Schmid, R.D.; Schomburg, D., J. Mol. Biol., **1993**, 229, 153-172.

4) Takegawa, K.; Fujiwara, K.; Iwahara, S.; Yamamoto, K.; Tochikura, T., Biochem.

Cell. Biol., **1989**, 67, 460-464.

5) Frederick, K.R.; Tung, J.; Emerick, R.S.; Masiarz, F.R.; Chamberlain, S.H.; Vasada, A.; Rosenberg, S.; Chakraborty, S.; Schopter, L.M.; Massey, V., J. Biol. Chem. **1991**, 389, 3793-3801.

6) Creighton, T.E., Proteins, Structure and Molecular Properties, W.H. Freeman and Co., N.Y., **1984**, 76

7) Kalisz, H.M.; Hecht, H-J.; Schomburg, D.; Schmid, R.D., Biochimica et Biophysica Acta, **1991**, 1080, 138-142.

8) Nakamura, S.; Hayashi, S.; Koga, K., Biochimica et Biophysica Acta, **1976**, 445, 294-308.

9) Smith, R.D.; Loo, J.A.; Charles, C.G.; Barinaga, C.J.; Vdseth, H.R., Anal. Biochem, **1990**, 62, 882-899.

10) Guzetta, A.W.; Basa, L.J.; Hancock, W.S.; Keyt, B.A.; Bennett, W.F., Anal. Chem., **1993**, 65, 2593-2962.

11) Feng, R.; Konishi, Y., Anal. Chem., **1992**, 64, 2090-2095.

12) Spackman, D.H.; Stein, W.H., Anal. Chem., **1958**, 30, 1190-1196.

13) Wilson, R.; Turner, A.P.F., Biosensors & Bioelectronics, **1992**, 7, 165-185.

14) Awad, W.I.; Hassan, S.M.; Zaki, M.T.M., Anal. Chem., **1972**, 44, 911.

15) Marshall, R.; Inglis, A.S., Methods Enzym., **1972**, 25, 54-63.

16) Badia, A.; Carlini, R.; Fernandez, A.; Battaglini, F.; Mikkelsen, S.R.; English, A.M., J. Am. Chem. Soc., **1993**, 115, 7054-7060.

17) Battaglini, F.; Koutroumanis, M.; English, A.M ; Mikkelsen, S.R., Bioconjugate

Chem. **1994**, 5, 430-435.

18) Trimble, R.B.; Maley, F., Biochem. Biophys. Res. Commun., **1977**, 78, 935-944.

3.0 Development of an Amperometric Enzyme Amplified Immunoassay

3.1 Introduction

An immunoassay is based on the use of an antibody (Ab) as a selective reagent for an antigen (Ag) or hapten, and therefore exploits the natural binding phenomena between an Ab paratope and an Ag epitope[1]. These assays offer high selectivity as well as high sensitivity[2]. The reaction is very selective because the epitope on the antigen will interact specifically with the antigen binding site on the antibody. Heterogeneous immunoassays require a separation step before the measurement can be taken whereas in a homogeneous immunoassay this step is not required[3].

The key to an immunoassay is to have a label to probe the antibody-antigen binding. The ideal immunoassay should have an inexpensive, safe and simple labelling procedure. The labelling should have minimal effects on the Ab-Ag binding and the label should be easily detected[4]. Either the antigen or the antibody can be labelled, and different types of labels have been used. The first labels to be introduced were radioisotopes, such as ^{125}I and ^{3}H, but the problem with these is that they are costly and hazardous, also inconvenient monitoring and disposal techniques are needed[5] Fluorescent and chemiluminescent labels were later introduced and examples of such labels are shown in Figure 3 1. Enzymes were first introduced as labels in the mid 1960s[5]. Alkaline phosphatase[6], tyrosinase[7] and glucose-6-phosphate dehydrogenase[2] are examples of enzyme labels. One advantage of enzyme labels is that the chemical amplification feature of the enzyme can be used[8]. This refers to the passage of a substrate through the catalytic cycle of an enzyme, generating multiple copies of the desired product. Other advantages are that enzyme labels are not a radiation hazard,

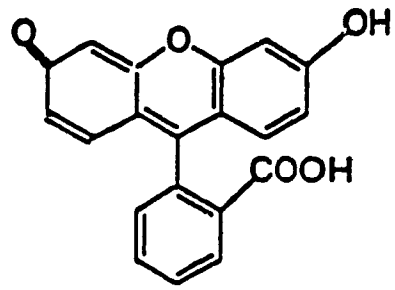

Fluorescein

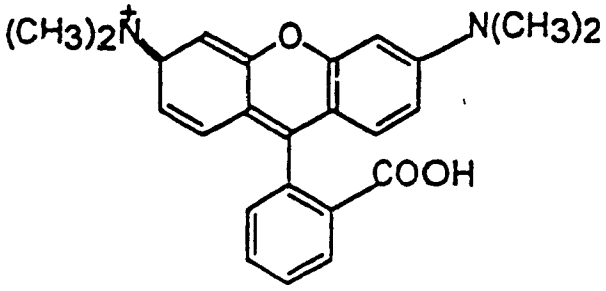

Tetramethylrhodamine

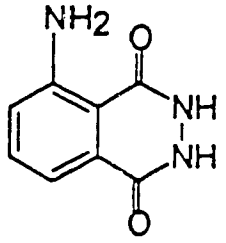

Luminol

Figure 3.1: Commonly used fluorescent (fluorescein and tetramethylrhodamine) and chemiluminescent labels (luminol) used in immunoassays.

the reagents have a long shelf life; and a rapid and simple change in product absorbance or fluorescence can be measured. The ideal labelling enzyme should have a high turnover number (k_{cat}), and the enzyme labelling should not interfere with the Ab-Ag binding. Detection limits using enzyme labels rival those of radioimmunoassays (10^{-15} M)[2].

Potentiometric or amperometric methods can be used for detection in electrochemical immunoassay. With potentiometry, a potential difference with respect to a reference electrode is measured, and the relationship between the concentration and signal is logarithmic. Amperometric measurements detect changes in current, therefore the relationship between the concentration and current is linear. An amperometric method of detection was chosen for this work. In oxidizing glucose to gluconolactone, the FAD centre in GOx is reduced to $FADH_2$ which can be reoxidized using a mediator, such as ferrocenecarboxylic acid (FCA) or ferrocenemethanol (FCOH). The reduced mediator can then be oxidized at an electrode surface as shown in Figure 3 2, to generate a current which is measured. Electrochemical methods employ rugged instrumentation which is very useful for field applications Sample turbidity, quenching and interference by chromophores and fluorophores in the analyte solution are problems often encountered with spectroscopic methods of detection but are avoided by using an electrochemical method Also, multiple electrochemical measurements can be made on the same sample whereas this is not the case if monitoring a change in absorbance, because a change in product concentration occurs throughout the solution. Using amperometric measurements, detection limits as low as 10^{-21} mole of immunoglobulin G (IgG) analyte were reported[21] The monitoring of digoxin, a cardioactive drug, in the blood of a patient is an example of an enzyme amplified

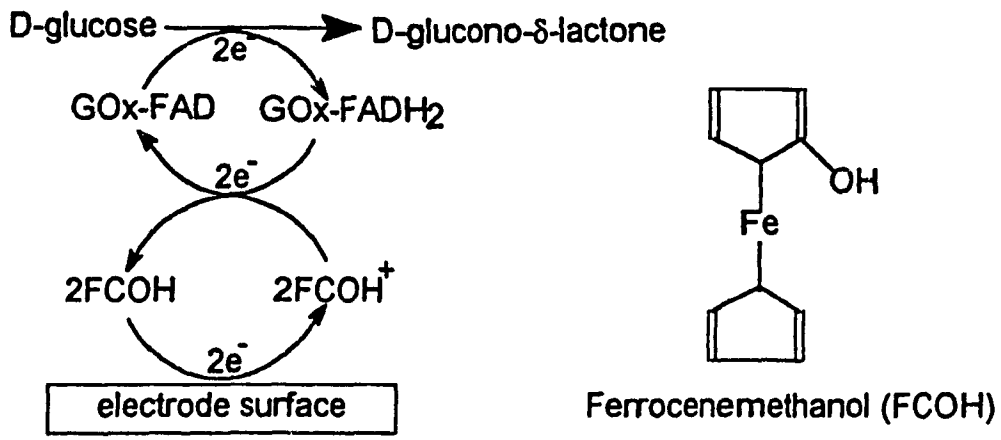

Figure 3.2: Electrocatalytic cycle of GOx using FCOH as an electron transfer mediator.

immunoassay that uses electrochemical detection[2]. The principle behind this type of assay is that when the Ab binds to its enzyme-labelled Ag, the enzyme loses activity. There is competition for Ab sites between free Ag and enzyme-labelled Ag; therefore, as the concentration of free Ag is increased in solution, the enzyme activity is restored. There are two conceivable modes of enzyme inactivation upon Ab binding. First, if the Ag is bound close to the active site of the enzyme, Ab binding could obstruct the active site making it impossible for the substrate to enter[10]. Access should also depend on the size of the substrate. Another possibility is that an allosteric mechanism causes a deformation or conformational change at the active site upon antibody binding, resulting in loss of activity[11].

The enzyme label used in this work in the development of a homogeneous enzyme amplified immunoassay is glucose oxidase (GOx). GOx is a dimeric glycoprotein with a molecular weight of 160 kD and has two tightly bound flavin adenine dinucleotides ($K = 1 \times 10^{10}$)[12]. GOx was chosen because it is stable, commercially available, relatively cheap and also the technology to covalently modify this enzyme with a hapten was in use in this laboratory[13] Two model analytes were chosen for the development of the immunoassay. fluorescein and 2,4-dinitrophenol. These analytes should compete with GOx-labelled fluorescein glycine amide (FGA) and 2,4-dinitrobenzoic acid (DNBA) for anti-fluorescein and anti-dinitrophenol binding sites, respectively. FGA and DNBA were covalently bound to GOx via EDC-NHS promoted amide bond formation, as described in Chapter 2.

FGA and DNBA were chosen as model analytes for two reasons. First of all, both polyclonal and monoclonal Abs to these haptens are commercially available. Secondly, as discussed in Chapter 2, DNBA and FGA are targeted to different residues on the protein, the

former haptens binds to GOx at its Lys residues, and the latter to its carboxylate residues. Since the Lys residues are further removed from the active site of GOx than the carboxylate residues, it was anticipated that FGA-modified GOx would undergo a larger change in activity upon Ab binding. Preliminary investigations of amperometric enzyme amplified immunoassays using GOx are presented in this chapter. The binding of monoclonal Ab to free FGA and FGA-GOx was characterized by fluorescence spectroscopy. Activity assays were then carried out spectrophotometrically and electrochemically to ascertain the effects of Ab binding to FGA-GOx and DNBA-GOx.

3.2 Experimental

3.2.1 Materials

2,4-Dinitrobenzoic acid (DNBA), monoclonal and polyclonal anti-dinitrophenol, (Anti-D; ~1.5 mg/ml) and monoclonal anti-fluoresceinisothiocyanate (Anti-F; ~3 mg/ml), ferrocenemethanol (FCOH) and guanidinium hydrochloride were purchased from Sigma. Fluorescein glycine amide (FGA) was obtained from Molecular Probes. $(FGA)_5$-GOx and $(DNBA)_x$-GOx were prepared as described in Sections 2.2.2.4 and 2.2.2.5, respectively. A BAS 100A potentiostat was used for electrochemical measurements. The glassy carbon electrode as well as the silver/silver chloride electrode (3 M KCl, E = 0.194 V vs NHE) were purchased from BioAnalytical Systems. Pt wire was used as an auxiliary electrode and was obtained from Fisher. Fluorescence measurements were carried out on a Shimadzu Model RF 5000 spectrofluorometer.

3.2.2 Methods

3.2.2.1 GOx Tryptophan Fluorescence under Native and Denaturing

Conditions: The fluorescence of the tryptophan (Trp) residues in unmodified GOx and in $(FGA)_5$-GOx was investigated under both native and denaturing conditions. Also, the Trp fluorescence of GOx in the presence of free FGA was investigated. Under native conditions the samples were in 0.1 M phosphate buffer, pH 7.0, and for denaturing conditions, 6 M guanidinium-Cl was added. In all cases the concentration of GOx used was 0.36 μM and, when present, the concentration of free FGA was 2 μM. The final volume in the fluorescence cuvette was 750 μl. To ensure complete denaturation, GOx samples were incubated with the denaturants at room temperature for 12 h before their fluorescence was measured. For consistent sample preparation, the samples in buffer were also left standing at room temperature overnight before recording their fluorescence. The absorbance of each sample at both the excitation and emission wavelengths was recorded to correct the observed fluorescence for inner-filter effects according to the following equation:

$$F_{corr} = F_{obs} * \text{antilog}\,(A_{ex} + A_{em})/2 \qquad (3.1)$$

where F_{corr} is the corrected fluorescence, F_{obs} the observed fluorescence, A_{ex} the absorbance at the excitation wavelength and A_{em} the absorbance at the emission wavelength[14].

3.2.2.2 Visible Fluorescence of Free FGA and $(FGA)_5$-GOx: Fluorescence of free FGA and $(FGA)_5$-GOx was investigated in 0.1 M phosphate buffer, and 6 M guanidinium-Cl was added to provide denaturing conditions when required. The absorbance at 489 nm of $(FGA)_5$-GOx and free FGA was matched to estimate the relative quantum yields The emission was measured from 495 to 600 nm. The buffer emission was substracted from that of the FGA samples and the emission intensities were corrected using eq 3 1.

3.2.2.3 Titration of free FGA fluorescence with anti-F : In all samples the concentration of FGA was 10 nM. The commercial stock solution of monoclonal anti-F was ~23 μM, and in the titration this was diluted with the 10 nM FGA solution. To ensure equilibration of the Ag-Ab interaction, the samples were placed at 4°C overnight before recording their fluorescence under the conditions given in Section 3.2.2.2.

3.2.2.4 Titration of $(FGA)_5$-GOx fluorescence with Anti-F: Aliquots of the commercial stock anti-F solution were added to $(FGA)_5$-GOx in 0.1 M phosphate buffer, pH 7.0. These solutions were diluted to give a final FGA concentration of 100 nM, and Ab concentrations between 0 to 500 nM The samples were left at 4°C overnight, and the fluorescence was measured under the conditions given in Section 3.2.2.2.

3.2.2.5 Preparation Ab:Modified-GOx Samples for the Electrochemical Assays: Aliquots of the commercial stock polyclonal anti-D (~10 μM) and monoclonal anti-F (~23 μM) solutions were added to the modified-GOx in the ratios given in Table 3.1. For the electrochemical assays the final concentration of both $(DNBA)_x$-GOx and $(FGA)_5$-GOx was constant at 4 μM. A control containing 4 μM native GOx in the presence of anti-D was prepared at a molar ratio of GOx:Ab of 1:0.1. The samples were stored at 4°C overnight before activity measurements were recorded.

3.2.2.6 Electrochemical Measurements of GOx Activity: Cyclic voltammetry was performed between -100 and 500 mV at a scan rate of 2 mV/s A standard three-electrode cell configuration, consisting of a glassy carbon working electrode, a silver/silver chloride reference electrode (3 M KCl, E = 0.194 V vs NHE) and a platinum auxiliary electrode, was used. The glassy carbon electrode (GCE) had a surface area of 0.071 cm^2 and was polished

Table 3.1: Molar ratios of modified- GOx and Ab.

# mol mod-GOx	# mol Ab
1.0	0
1.0	0.05
1.0	0.1
1.0	0.3
1.0	0.5
1.0	1.0

with 0.05 μm alumina and sonicated in distilled water for 5 min prior to use. FCOH was used as an electron-transfer mediator, and a stock solution of 88 μM in 0.1 M phosphate buffer (pH 7.0) was prepared. Cyclic voltammograms of the enzyme plus mediator were first recorded, and then glucose, from a stock solution of 1 M in water, was added to record the catalytic currents.

3.3 Results

3.3.1 GOx Tryptophan Fluorescence under Native and Denaturing Conditions:

The results obtained under native conditions are shown Table 3.2 whereas those obtained under denaturing conditions are found in Table 3.3, and the corresponding fluorescence spectra are shown in Figure 3.3.

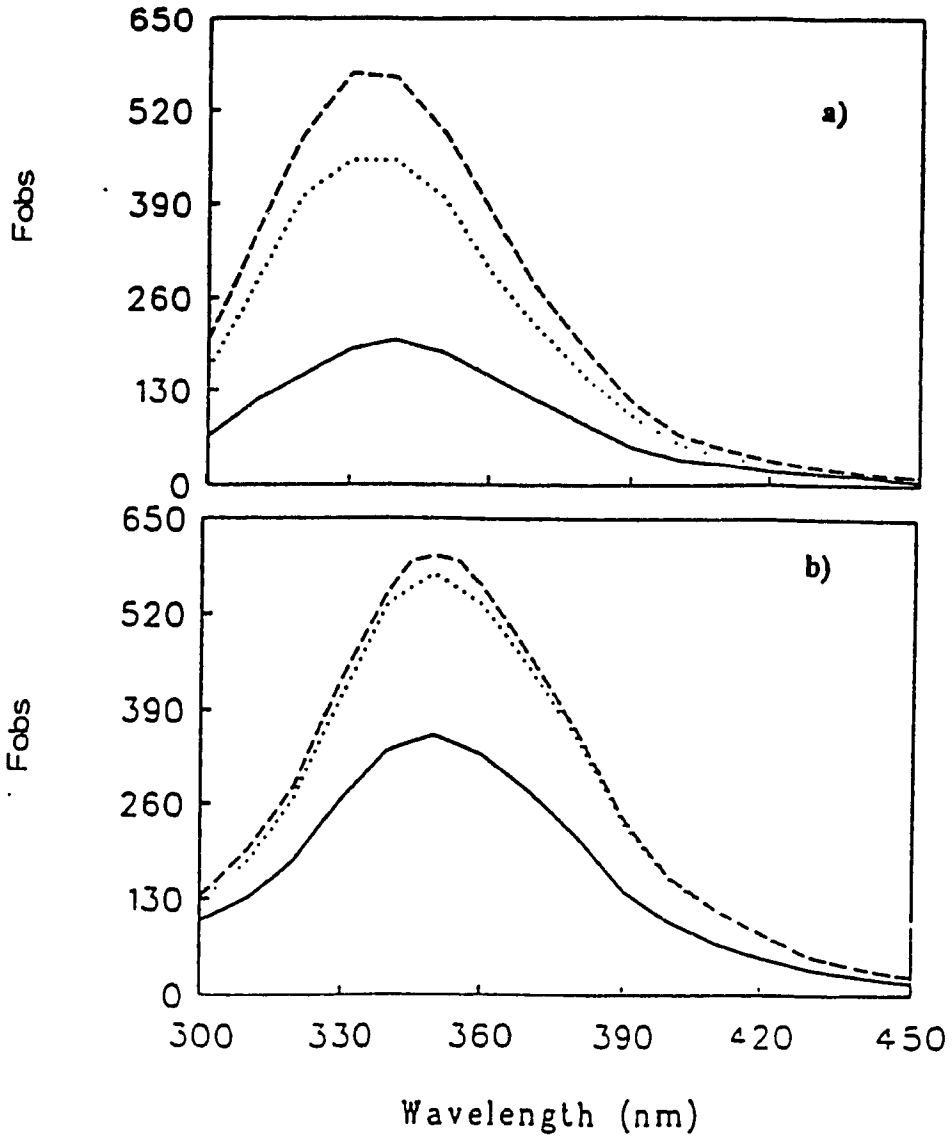

Figure 3.3: Trp fluorescence emission spectra obtained for GOx (- - - -), a noncovalent mixture (1 : 5) of FGA and GOx (....), and $(FGA)_5$-GOx (——) in (a) 0.1 M phosphate buffer, pH 7.0, and (b) 6 M guanidinium-Cl. The excitation wavelength was 280 nm and the slits were 5 nm for both excitation and emission. The concentration of GOx was 0.36 μM in all the samples.

Table 3.2: Fluorescence of Tryptophan residues in GOx in buffer[a]

Sample	λ_{max} (nm)	F_{corr}	% F
GOx	333.6 ± 1	582 ± 3	100
$(FGA)_5$-GOx	336.8 ±1	201 ± 2	34
GOx + FGA	333.6 ±1	463 ± 2	79

[a] Experimental conditions: Excitation wavelength, 280 nm; emission recorded between 300 and 450 nm; slits 5 nm for both excitation and emission. Samples were in 0.1 M phosphate buffer, pH 7.0, and they were left at room temperature for 12 h. before recording their fluorescence intensities.

Table 3.3: Fluorescence of Tryptophan residues in GOx 6 M guanidinium-Cl[a]

Sample	λ_{max} (nm)	Fluorescence Intensity	% F
GOx	350.4 ± 0.5	602 ± 1	100
$(FGA)_5$-GOx	350.4 ± 0 5	357 ±3	66
GOx + FGA	350.4 ± 0.5	574 ±1	99

[a] Experimental conditions as in footnote to Table 3.2 except 6 M guanidinium-Cl was added to the samples.

As can be seen from the tables, the fluorescence maximum is red-shifted upon exposure of GOx to the denaturant as expected, since the Trp residues are exposed to the aqueous environment when the protein is denatured. The fluorescence is quenched when

FGA is present, but the quenching is far greater for $(FGA)_5$-GOx than for the noncovalent mixture. Furthermore, under denaturing conditions, the quenching is relieved in the noncovalent mixture but significant quenching is still observed for $(FGA)_5$-GOx. This provides strong evidence for covalent modification, since the quenching would have been relieved upon denaturation of the protein, if the FGA molecules were only trapped in the enzyme. The fact that the quenching was not relieved indicates that in denatured $(FGA)_5$-GOx the FGA molecules are still close enough to the Trp residues for efficient energy transfer to occur. However, the fluorescence intensity for $(FGA)_5$-GOx relative to unmodified GOx is greater under denaturing conditions, indicating that the average Trp-FGA distance is greater in the denatured form of $(FGA)_5$-GOx as expected.

3.3.2 Fluorescence of Free FGA and $(FGA)_5$-GOx: The visible fluorescence of free FGA and $(FGA)_5$-GOx was compared for samples with the same absorbance at the excitation wavelength (489 nm). The observed fluorescence intensities are given in Tables 3.4 and 3.5 and the spectra are given in Figure 3.4.

Table 3.4: FGA fluorescence in buffer[a]

Sample	λ_{max} (nm)	%F
Free FGA	512 ± 1	100
$(FGA)_5$-GOx	516 ± 1	29

[a] Experimental conditions: excitation wavelength 489 nm; emission recorded between 495 and 600 nm; slits 1.5 nm for both excitation and emission. Samples were in 0.1 M phosphate buffer, pH 7.0.

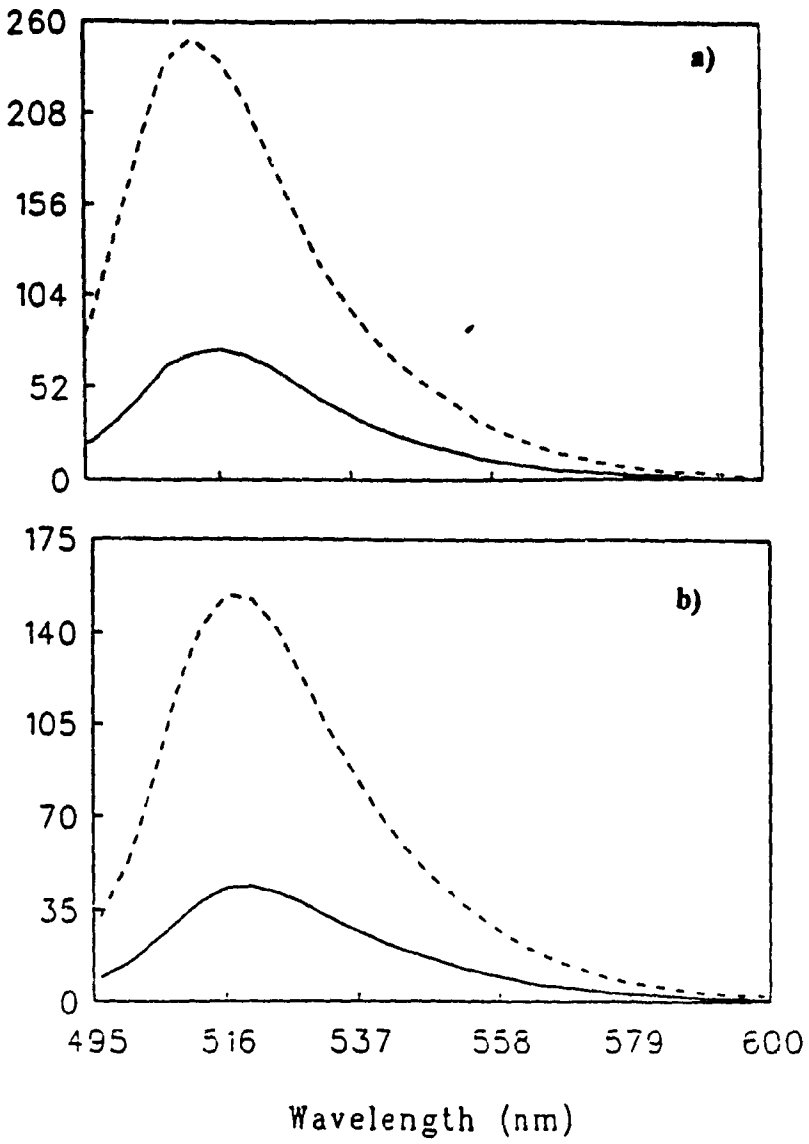

Figure 3.4: Fluorescence spectra for free FGA (---) and $(FGA)_5$-GOx (—) in a) 0.1 M phosphate buffer, pH 7.0, and b) 6 M guanidinium-Cl. The absorbance of the samples was matched at 489 nm prior to the fluorescence measurements. The excitation wavelength was 489 nm and the slits were 1.5 nm wide for both excitation and emission

Table 3.5: FGA Fluorescence in 6M guanidinium-Cl[a]

Sample	λ_{max} (nm)	%F
Free FGA	517 ± 1	100
$(FGA)_5$-GOx	518 ± 1	28

[a] Experimental conditions as in footnote to Table 3.4 except 6 M guanidinium-Cl was added to the samples.

The data in the tables reveal that the emission of FGA is red-shifted when it is covalently bound to GOx, and also in denaturant. Since the emission of FGA is strongly dependent on the protonation state of the xanthenone enolic moiety (which has a pKa of ~6.7 for unsubstituted fluorescein), binding of the fluorophore to GOx or its addition to guanadinium-Cl may alter the pKa of this moiety, resulting in the observed fluorescence red-shift. The data also reveal strong quenching of FGA fluorescence on binding to GOx under both native and denaturing conditions. This quenching may be due to some steric interaction between the fluorophore and GOx which decreases the fluorescence quantum yield of the former.

3.3.3 Titration of Free FGA fluorescence with Anti-F Concentration: Binding of fluorescein and its derivatives to Ab results in a decrease in fluorescence[15]. In this set of experiments, the fluorescence was measured relative to 10 nM free FGA in the absence of anti-F. In Figure 3.5(a), the FGA fluorescence is plotted versus concentration of anti-F binding sites. This plot was obtained by averaging the results from 4 independent trials. In

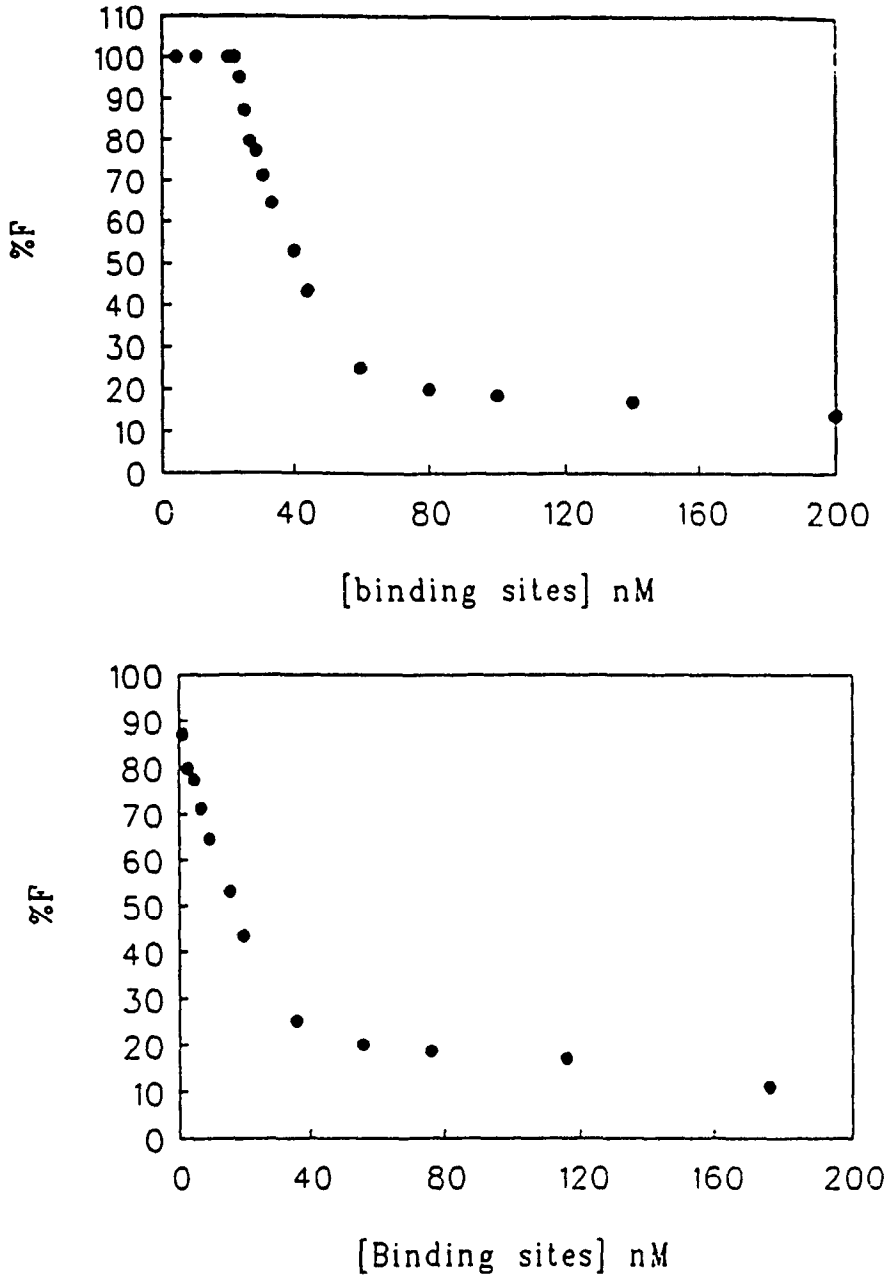

Figure 3.5: Titration of free FGA fluorescence with monoclonal Anti-F. (a) Observed data and (b) corrected data (see text). The %F for 10 nM free FGA in the absence of anti-F was taken as 100%. The samples were in 0.1 M phosphate buffer, pH 7.0. The excitation wavelength was at 489 nm, the emission was recorded between 495 and 600 nm, and the slits were 5 nm for both excitation and emission.

each trial it was observed that no fluorescence quenching occurred at anti-F binding site concentrations less than ~ 24 nM. This suggests that at low nM concentrations the Ab may have been adsorbed to the surface of the cuvette. Thus, to estimate a Kd from the data in Figure 3 5(a) 24 nM binding sites were substracted from the total binding site concentration. This plot is shown in Figure 3.5(b). From the plot in Figure 3.5(b) it appears that Kd < 10 nM, the concentration of FGA, since the shape of the titration curve approaches that expected for stoichiometric binding, which requires Kd << [FGA]. Thus, from Figure 3.5(b) Kd can be estimated from the concentration of binding sites that gives half maximal quenching %F levels off at ~14 and the binding site concentration at half maximal quenching (%F = 43) is ~ 12 nM which is a rough estimate of Kd The high quenching (86%) on FGA binding to anti-F is similar to the ~90% quenching reported for fluorescein binding to a number of its monoclonal Abs Also, the estimated Kd of 12 nM is within the range of Kds reported for Ab-fluorescein binding (10 μM-0.1 nM)[15].

3.3.4 Titration of $(FGA)_5$-GOx Fluorescence with Anti-F: The titration of $(FGA)_5$-GOx with anti-F was performed with a FGA concentration of 100 nM From the titration curve, which is shown in Figure 3 6, it is apparent that anti-F binds GOx-bound FGA much less tightly than free FGA For example, at a binding site concentration of 200 nM very little quenching of FGA fluorescence is observed in Figure 3.6, whereas in Figure 3.5(b) maximal quenching is observed at a binding site concentration < 200 nM. Furthermore, it appears from Figure 3 6 that the fluorescence of GOx-bound FGA is quenched to a much lesser extent on anti-F binding compared to free FGA, since the former is beginning to level off at %F~55% Assuming that the fluorescence of anti-F-bound $(FGA)_5$-GOx levels off

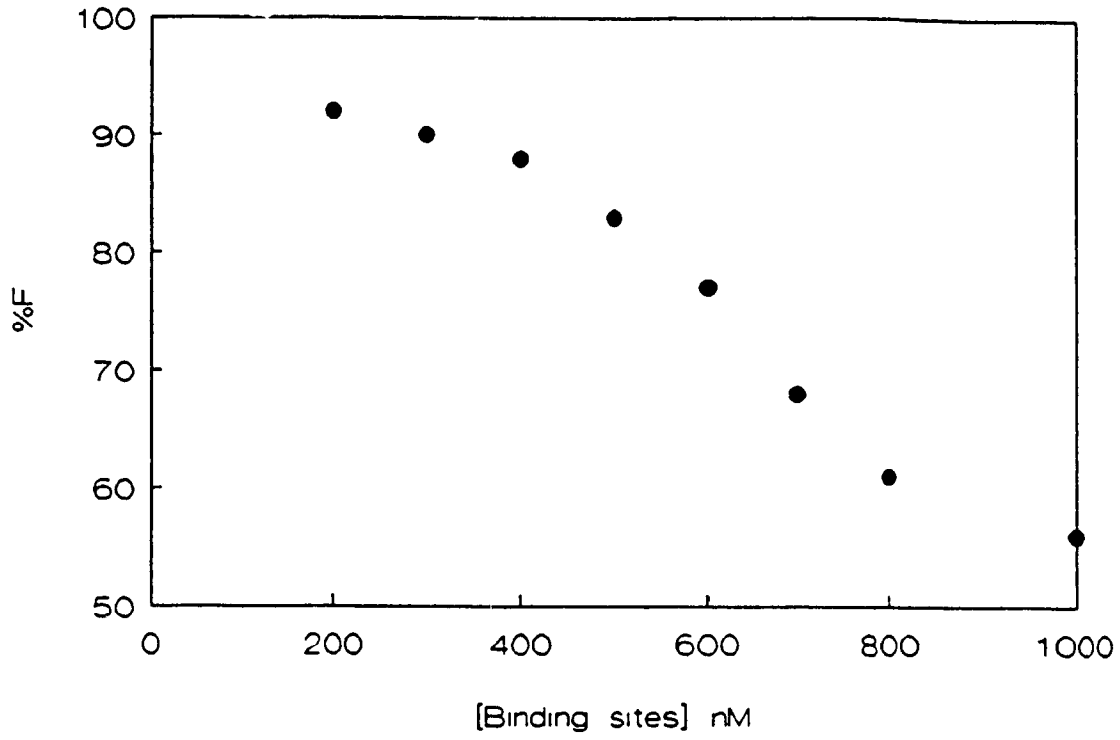

Figure 3.6: Titration of the fluorescence of $(FGA)_5$-GOx with monoclonal anti-F. The same concentration of $(FGA)_5$-GOx in the absence of anti-F was assumed to have 100 % fluorescence. The samples were in 0.1 M phosphate buffer, pH 7 0 The excitation wavelength was 489 nm and the emission was recorded between 495 and 600 nm The slits were 5 nm for both excitation and emission

at %F ~ 50, then the binding site concentration at half maximal quenching would be ~600 nM. This suggests that the Kds for anti-F binding to free and GOx-bound FGA may differ by as much as a factor of 50.

3.3.5 Electrochemical Measurements of $(FGA)_5$-GOx Activity: Studies of mediator-GOx electron-transfer kinetics can be performed by voltammetry. The mediator is continuously produced at working electrode surface when the applied potential is positive of the mediator's formal reduction potential. Under these conditions, reduced GOx reacts with the mediator near the electrode surface, generating oxidized enzyme and the reduced form of the mediator. Reoxidation of the mediator at the working electrode generates the catalytic current, which is related to the enzyme activity. Catalytic currents were obtained for different samples of $(FGA)_5$-GOx with and without anti-F. In all samples the concentration of enzyme was 4 μM. The GOx to anti-F ratios given in Table 3.6 were employed in the electrochemical measurements. The Ab concentrations correspond to binding site concentrations which are 1.3 to 7 times greater than the Kd estimated for anti-F binding to $(FGA)_5$-GOx above. The catalytic currents obtained are also found in Table 3.6 and examples of the cyclic voltammograms recorded before and after the addition of glucose are shown in Figure 3.7.

As can be seen from Table 3.6, the activity of $(FGA)_5$-GOx is lower than that for native GOx in the heterogeneous assay. This was expected since, as indicated in Chapter 2, $(FGA)_5$-GOx exhibits lower activity than native GOx in the homogeneous activity assay. However, no significant further loss of activity was observed upon addition of anti-F, although at the Ab concentrations used binding of anti-F to $(FGA)_5$-GOx is expected. Thus,

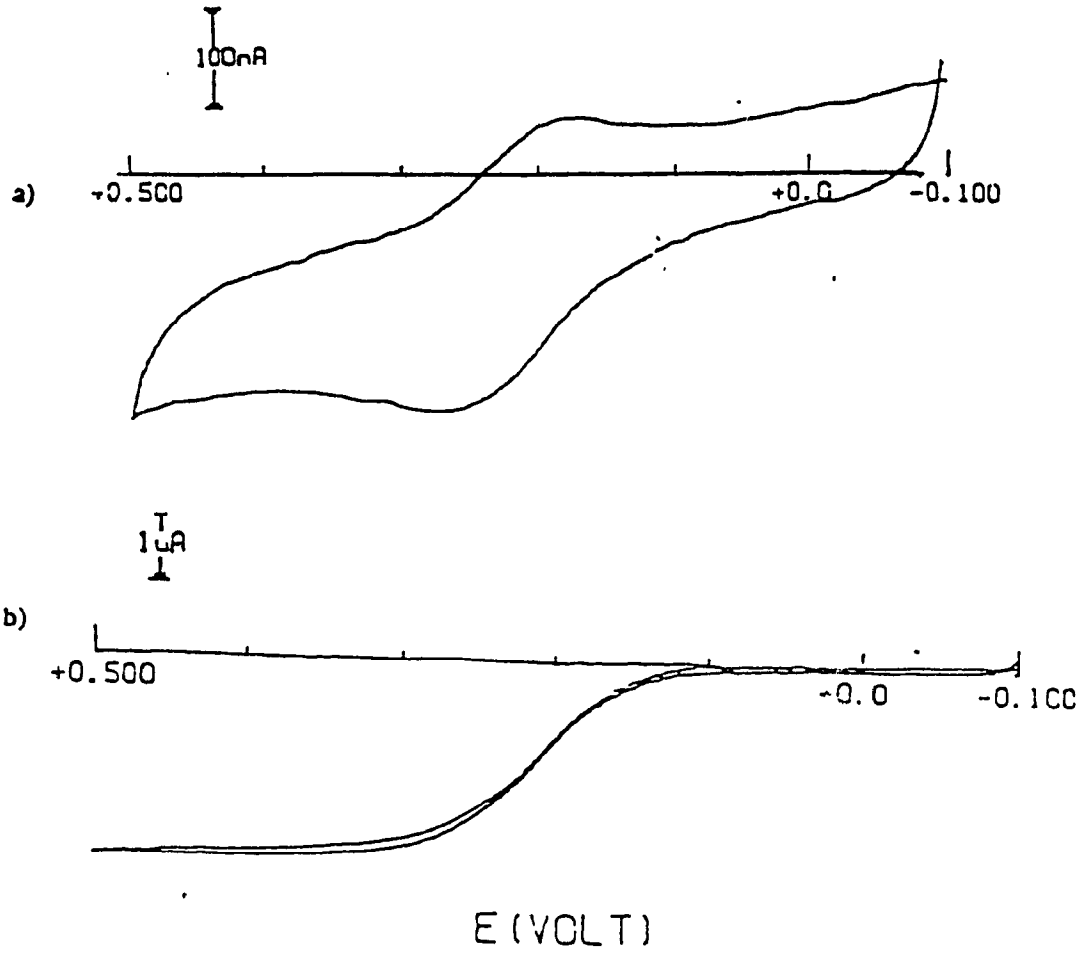

Figure 3.7: Cyclic voltamograms of 44 μM FCOH in the presence of 4 μM FGA-GOx (a) before and (b) after the addition of 55 mM glucose at a glassy carbon electrode with an Ag/AgCl reference electrode (3 M KCl, E = 0.194 V vs NHE) and a platinum wire auxiliary electrode. The potential was scanned from -100 mV to 500 mV at a scan rate of 2 mV/s

Table 3.6: Catalytic currents obtained for different ratios of $(FGA)_5$-GOx to Ab[a]

Sample	E:Ab ratio	i_{cat} (μA)
GOx	1:0	3.6
$(FGA)_5$-GOx	1:0	2.7
$(FGA)_5$-GOx	1:0.1	2.3
$(FGA)_5$-GOx	1:0.3	2.3
$(FGA)_5$-GOx	1:0.5	2.2

[a] 4 μM native GOx is used as a control

it can be postulated that the residues modified with FGA are not sufficiently close to the active site for anti-F binding to reduce mediator accessibility to this site. Heterogeneous assays were also carried out with a FGA-GOx sample, which was received from Dr. Battaglini of our laboratory, and which had been modified with 14 FGA per GOx. This modified-GOx sample was prepared by periodate oxidation of the carbohydrate moiety and binding of FGA to the aldehyde groups produced. The catalytic currents obtained with $(FGA)_{14}$-GOx in the presence and absence of anti-F are shown in Table 3.7.

The $(FGA)_{14}$-GOx sample shows less than 50% heterogeneous activity compared to native GOx, and this is consistent with the results from homogeneous activity assays. However, the addition of anti-F did not further reduce the activity of $(FGA)_{14}$-GOx as was observed for $(FGA)_5$-GOx. Therefore, it must be concluded that anti-F binding to $(FGA)_{14}$-GOx does not obstruct access of the FCOH mediator to the active site of the enzyme.

Table 3.7: Catalytic currents obtained with $(FGA)_{14}$-GOx with and without anti-F[a]

Sample	E:anti-F ratio	i_{cat} (μA)
GOx	1:0	3.5
$(FGA)_{14}$-GOx	1:0	1.61
$(FGA)_{14}$-GOx	1:0.5	1.62
$(FGA)_{14}$-GOx	1:1	1.66

[a] Experimental conditions used were the same as in Table 3.6

3.3.6 Electrochemical Measurement of $(DNBA)_x$-GOx Activity: The number of DNBA molecules bound to GOx was not determined, therefore the ratios of $(DNBA)_x$-GOx to anti-D chosen were based on those used for $(FGA)_5$-GOx. The results are compared to native GOx, and the activity of a control containing native GOx in the presence of anti-D was also measured in order to determine whether anti-D interferes with the assay. The results are shown in Table 3.8.

Upon addition of 0 1 molar equivalent of anti-D to the $(DNBA)_x$-GOx there is a drop in activity, but no further decrease was observed at higher anti-D concentrations. The presence of a precipitin when the $(DNBA)_x$-GOx:anti-D ratio was 1:1 or higher is consistent with the presence of covalently-bound DNBA on GOx. Furthermore, it is anticipated that precipitin formation would be promoted by the presence of a number of DNBA groups per GOx molecule.

Table 3.8: Catalytic currents obtained for $(DNBA)_x$-GOx in the absence and presence of monoclonal anti-D[a,b]

Sample	E:Ab ratio	i_{cat} (μA)[c]
GOx	1:0	3.63 ±0.3
GOx	1:0.1	3.58 ±0.5
$(DNBA)_x$-GOx	1:0	2.83 ±0.4
$(DNBA)_x$-GOx	1:0.1	2.66 ±0.5
$(DNBA)_x$-GOx	1:0.3	2.63 ±0.5
$(DNBA)_x$-GOx	1:0.5	2.61 ±0.7

[a] Experimental conditions were the same as in Figure 3.7

[b] A precipitin was observed when the E:Ab ratio was 1:1

[c] The data are the average of two to four trials

3.4 Discussion

The results of the Trp fluorescence experiments on unmodified GOx and $(FGA)_5$-GOx under both native and denaturing conditions provide strong evidence that GOx has been covalently modified with FGA. This arises from the fact that quenching of Trp fluorescence by FGA is not relieved upon denaturation of the modified GOx (Table 3.3), but quenching was relieved for the noncovalent mixture (Table 3.2). If FGA had been simply entrapped within the enzyme matrix or adsorbed onto its surface, it would have been released on denaturation of GOx. The release of noncovalently bound FGA molecules into the aqueous solvent would have relieved the quenching, but this was not observed since the fluorescence

of $(FGA)_5$-GOx is significantly lower than that of unmodified GOx in 6 M guanadinium-Cl. The residues on GOx that were covalently modified with FGA were not determined in this study. This would require tryptic digestion of the modified protein followed by analysis of the peptides by ES-MS or by carrying out amino acid analysis.

As can be seen from Figure 3.4 and the results in Tables 3.4 and 3.5, the fluorescence of FGA is considerably changed upon conjugation to GOx. A sharp decrease in fluorescence intensity of $(FGA)_5$-GOx relative to free FGA was observed in both buffer and 6 M guanadinium-Cl, suggesting that the FGA molecules were altered upon covalent attachment to the enzyme. As previously mentioned, this may be caused by perturbation of the fluorophore on binding to the large GOx (160 kD) molecule. Another possibility is that the conversion of the amino group on FGA to an amide group, which is strongly electron withdrawing, may change the electronic properties of the FGA fluorophore. However, considering that the amino group is four bonds removed from the phenyl ring, the electron withdrawing effects of an amide at this position should be only weakly transmitted to the ring structure. In addition to quenching, the emission maximum red-shifts by ~4 nm on FGA binding to GOx. As mentioned above this could be due to a change in the pKa of the enolic group which has a pKa of 6.7 in free fluorescein

From the FGA fluorescence titrations with anti-F shown in Figures 3 5 and 3.6, it is apparent that GOx-bound FGA has much lower affinity for the Ab. The anti-F used in these experiments was raised against protein-conjugated FITC, and the conjugation of both FITC and FGA to a protein is compared in Figure 3.8. As can be seen from this figure, the FITC- and FGA-protein immunogens are identical except for the spacer group between the

a)

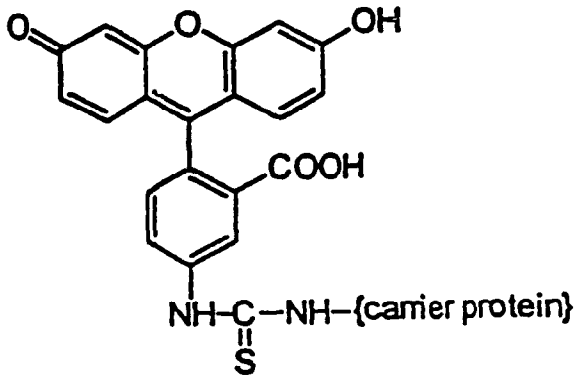

b)

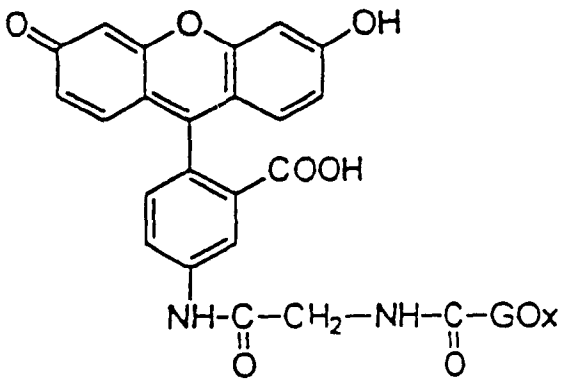

Figure 3.8: Structure of the fluorescein moiety of the FITC immunogen (a) and (b) (FGA)-GOx

fluorescein moiety and the protein. Since anti-fluorescyl Abs exhibit essentially no cross-reactivity with rhodamine compounds, this suggests that the xanthonyl ring is the immunodominant portion of the fluorescein molecule[15]. Hence, the low reactivity of anti-F with $(FGA)_5$-GOx observed here is somewhat surprising. It is speculated that the carbohydrate moiety of GOx may interfere with the FGA-anti-F interaction.

The results shown in Table 3.6 reveal very little change in the electrochemically determined enzyme activity of $(FGA)_5$-GOx upon addition of anti-F. Since the anti-F concentration in these samples is estimated to be above the Kd values for anti-F binding to $(FGA)_5$-GOx, the assay results imply that Ab binding does not reduce the access of FCOH to the active site of GOx. The results also indicate that anti-F binding does induce any conformational change in the enzyme that would lead to activity loss.

Electrochemical activity was also determined for $(DNBA)_x$-GOx in the presence of both polyclonal and monoclonal anti-D. As found for $(FGA)_5$-GOx, antibody binding to $(DNBA)_x$-GOx does not have a significant effect on enzyme activity as can be seen from the data in Table 3.8.

The electrochemical assay results show that Ab binding to GOx covalently modified with haptens does not significantly affect enzyme activity Significant changes in activity upon Ab binding are desirable for immunoassays. Since mediator access to the active site is essential for efficient electrochemical enzyme activity, a possible strategy to reduce access in the presence of bound Ab is to increase the size of the mediator. With this goal in mind, the activity of GOx using cytochrome c as an electron-acceptor substrate is presented in the next chapter.

3.5 References

1) McClintock, S.A.; Purdy, W.C., Electrochemical Sensors in Immunological Analysis, Ngo, T.T., Ed., Plenum Press, New York, **1987**, 77.

2) Wright, S.D.; Halsall, B.H.; Heineman, W.R., Electrochemical Sensors in Immunological Analysis, Ngo, T.T., Ed., Plenum Press, New York, **1987**, 117.

3) Campbell, A.M., Laboratory Techniques in Biochemistry and Molecular Biology, **1991**, 350.

4) Foulds, N.C.; Frew, J.E.; Green, M.J., Biosensors, a Practical Approach, Cass A.E.G., Ed., **1990**, 100.

5) Tijssen, P., Laboratory Techniques in Biochemistry and Molecular Biology Vol 15, Practice and Theory of Enzyme Immunoassays, Burdon, R.H.; van Knippenberg, P.H., Ed., Elsevier, Amsterdam, **1985**, 1.

6) Thompson, R.Q.; Barone III, G.C.; Halsall, H.B.; Heineman, W.R., Anal. Biochem., **1991**, 192, 90.

7) Rechnitz, G.A., Anal. Chem., **1993**, 65, 380-85.

8) Blaedel, W.J.; Boguslaski, R.C., Anal.Chem., **1978**, 50, 1026-1032.

9) Jenkins, S.; Halsall, H.B.; Heineman, W.R., J. Res. Natl. Stand., **1988**, 93, 491.

10) Heineman, W.R.; Halsall, H.B., Anal Chem, **1985**, 57, 1321A-1330A.

11) Ngo, T.T.; Electrochemical Sensors in Immunological Analysis, Ngo, T.T., Ed., Plenum Press, New York, **1987**, 103.

12) Wilson, R .; Turner, A.P.F., Biosensors & Bioelectronics, **1992**, 7, 195-185.

13) Badia, A.; Carlini, R.; Fernandez, A.; Battaglini, F.; Mikkelsen, S.R.; English, A.M.,

J. Am. Chem. Soc., **1993**, 115.

14) Lakowicz, J.R., Principles of Fluorescence Spectroscopy, Plenum Press, New York, **1983**.

15) Herron, J.N.; Kranz, D.M.; Jameson, D.M.; Voss, E.W., Biochemistry, **1986**, 25, 4602-4609.

4.0 Cytochrome c as an Electron-Acceptor Substrate for Glucose Oxidase

4.1 Introduction

Molecular oxygen is the natural electron acceptor in the glucose oxidase (GOx) catalytic cycle. Many studies, however, have shown that a variety of low molecular weight oxidants can be used *in vitro* as alternative electron acceptors. These mediator species include one-electron acceptors such as ferrocene derivatives[1,2] and osmium complexes[3] and two-electron acceptors such as quinones[4] and phenothiazine[5] derivatives. From the results of these studies, it was observed that positively-charged species are more effecient mediators for GOx.

Cytochrome c (cyt c) is a positively-charged 12 kD heme protein whose function is electron transport in mitochondrial respiration. It was speculated that the use of a large mediator such as cyt c may give rise to differential activity for modified-GOx in the presence and abscence of Ab. Little or no change in activity was observed in the previous chapter when anti-D or anti-F were added to modified-GOx using the small mediator FCOH.

Cyt c has been found to give an irreversible or nonexistent voltammetric response at noble metal electrodes such as platinum (Pt) and gold (Au)[6]. It was reported that chemical pretreatment of these electrodes[7,8] results in an enhanced rate of heterogeneous electron transfer, but the signal was not long-lived. The use of indium oxide and tin oxide semiconductor electrodes provided one of the first instances of direct quasi-reversible electrochemistry of cyt c[9]. Extensive research has been done on the modification of Au electrode surfaces by the chemisorption of 4,4'-bipyridyl[6] or other modifiers[10] , as well as the use of semiconductor[11,12] electrodes, as a means to achieve quasi-reversible electrochemistry

of cyt c. Surface modification of an Au electrode by chemisorption has proved to be a simple yet effective method for the promotion of direct electron transfer between cyt c and the electrode surface. The modifiers must contain nitrogen, sulfur or phosphorus atoms for chemisorption onto Au to occur. The modifiers must also have a functional group that can interact with the protein, to provide a favourable orientation for electron transfer. Since cyt c is positively charged around its heme edge, carboxylate or phosphate functional groups in the modifiers promote interaction of cyt c with the electrode surface[6].

The amino acid cysteine (Cys) chemisorbs to Au electrodes through its thiol group, and its carboxylate group can interact with the Lys residues in cyt c. With this system, the electrochemistry of cyt c was quasi-reversible and persistent[14]. This work examines the use of cyt c as a substrate for GOx. The activity of the enzyme with ferricyt c as an electron acceptor was studied spectrophotometrically and electrochemically. Commercial horse heart cyt c contains polymeric denatured forms[15] as well as deaminated forms[16] and must be purified if electrode fouling is to be avoided[17,18]. Cys and 3-mercaptopropionic acid (Figure 4.1) were used to promote electron transfer from cyt c to the Au electrodes and the results are presented for mediated GOx activity using voltammetry at Au electrodes modified with these thiol compounds.

4.2 Experimental

4.2.1 Material

Glucose oxidase from *Aspergillus niger* (GOx, E.C. 1.1.3.4, Grade II, lyophilized powder), was purchased from Beohringer Mannheim, and horse heart cytochrome c (cyt c, Type III and IV), bis(2-Hydroxyethyl)imino-tris(hydroxymethyl)methane,

(a)

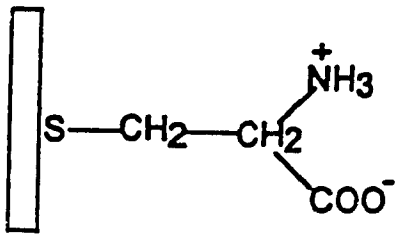

(b)

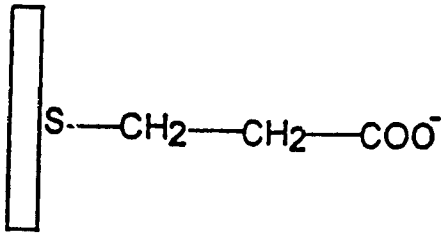

Figure 4.1: Structure of a) L-cysteine and b) 3-mercaptopropionic acid modified Au electrode

$(HOCH_2CH_2)_2NC(CH_2OH)_3$ (bis-tris) and mineral oil were obtained from Sigma. 3-Mercaptopropionic acid, L-cysteine hydrochloride, stearic acid and α-D-glucose were purchased from Aldrich. A stock solution of glucose (1 M) in distilled water was left to mutarotate at 4 °C overnight. Mono- and dibasic sodium phosphate, potassium ferricyanide and potassium chloride were obtained from Fisher. Carbon powder was obtained from Johnson Matthey.

Sephadex G-25 fine grade, molecular exclusion gel, a Mono S HR 10/10, cation exchange column and CM-Sepharose CL 6B cation-exchange gel were obtained from Pharmacia, who also provided the FPLC system. This was controlled by a LC-500 unit connected to two P-500 pumps, a UV-M monitor and a MV-7 motorized valve for sample injection All FPLC mobile phases were prepared with nanopure water (specific resistance 18 MΩcm) from a Barnstead Nanopure system, filtered through a 0.45-μm membrane filter (Gelman Sciences) and degassed by sonication or vacuum prior to use An ultrafiltration cell with YM 30 or YM 5 filters (MW cutoffs 30 kD and 5 kD, respectively) were purchased from Amicon. All absorbance measurements were performed on a Helwett Packard 8451A diode array spectrophotometer or a Beckman DU650 spectrophotometer A BAS 100A potentiostat was used for electrochemical measurements Gold and glassy carbon electrodes as well as a silver/silver chloride electrode (3 M KCl, E = 0 194 V vs NHE) and a carbon paste electrode holder were purchased from BioAnalytical Systems. Pt wire was used as an auxiliary electrode and was obtained from Fisher

4.2.2 Methods

4.2.2.1 Small-Scale Purification of Cytochrome c: Horse heart cyt c was purified

by cation-exchange chromatography on a Mono S 10/10 FPLC column equilibrated with 20 mM sodium phosphate buffer, pH 7.0. Cytochrome c (500 µl of 15 to ~30 mg/ml solution) in 20 mM sodium phosphate buffer, pH 7.0, was injected onto the column and elution was carried out with a gradient of 0 to 0.6 M KCl at a flow rate of 1.0 ml/min. The absorbance was followed at 280 nm, and 5 ml fraction were collected. Commercial cyt c contains denatured[15] and deaminated forms[16] (Gln→Glu and Asn→Asp). Since native cyt c is more positively charged, it is retained longer on a cation-exchange column than the deaminated forms. The chromatogram obtained for commercial horse heart cyt c is shown in Figure 4.2. As can be seen, the proteins were eluted at a high mobile phase salt concentration. The deaminated forms were eluted first, followed by the native form which was eluted at 0.44 M KCl The fractions corresponding to native cyt c (elution volume 24-25 ml) were pooled and concentrated using an ultrafiltration cell (YM 5) and the absorbance was measured at 410 nm.

4.2.2.2 Large Scale Purification of Cytochrome c : 50 - 100 mg of horse heart cyt c were dissolved in 2 -3 ml of water To ensure that all the iron present was in the Fe(III) form, 1-3 mg of potassium ferricyanide was added to the solution. The cyt c was purified on a CM Sepharose Cl 6B column (1 5 x 60 cm). Prior to addition of the sample, the column was equilibrated with 100 mM phosphate buffer, pH 7.0 The protein was allowed to elute overnight at a flow rate of 25 ml/hr, and 5 ml fraction were collected. The absorbance of each fraction was measured at 280 and 410 nm, and fractions with an A_{410}/A_{280} ratio greater than 4.5 were pooled and concentrated by ultrafiltration using a stirred Amicon cell (50 ml) with a YM 5 filter The chromatogram obtained for the purification of cyt c using cation-exchange chromatography is shown in Figure 4 3. The first sharp band is due to potassium

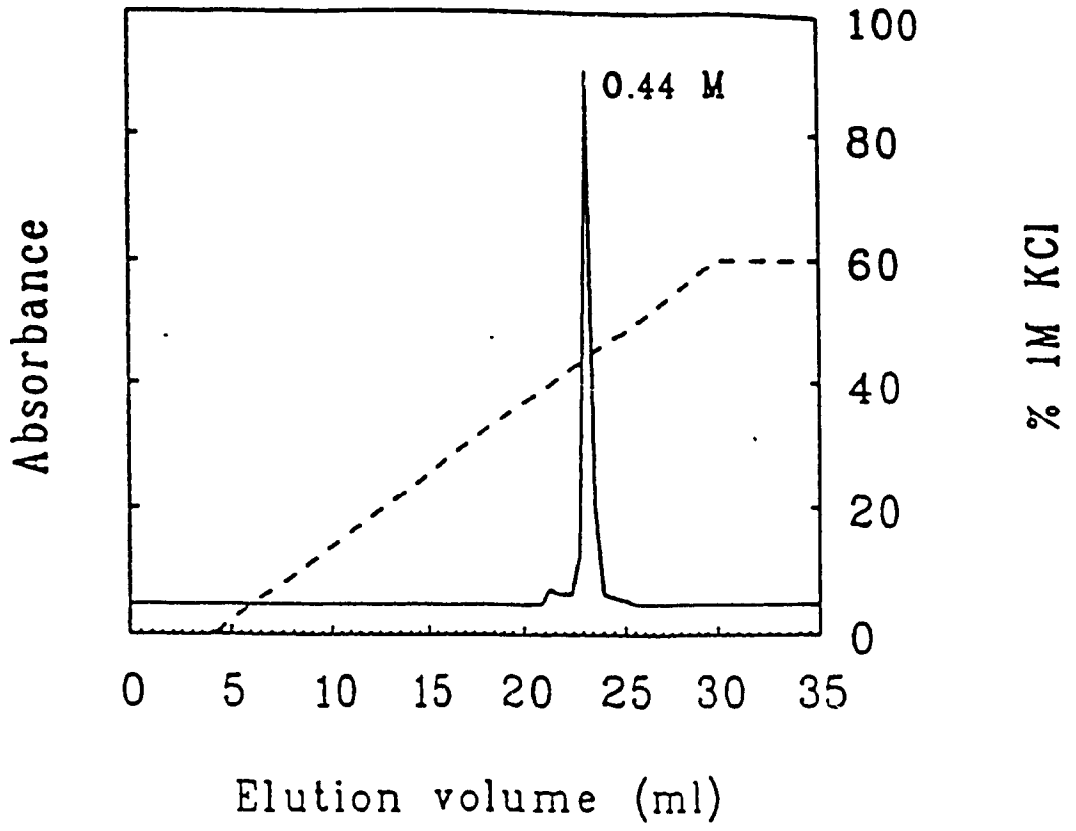

Figure 4.2: FPLC cation-exchange chromatography (Mono S, HR 10/10) of 500 µl of 30 mg/ml of cyt c. The column was equilibrated with 20 mM phosphate buffer, pH 7 0 and elution was with a gradient of 0 to 0.6 M KCl at a flow rate of 1.0 ml/min Absorbance was followed at 280 nm, and the fraction size was 5 ml.

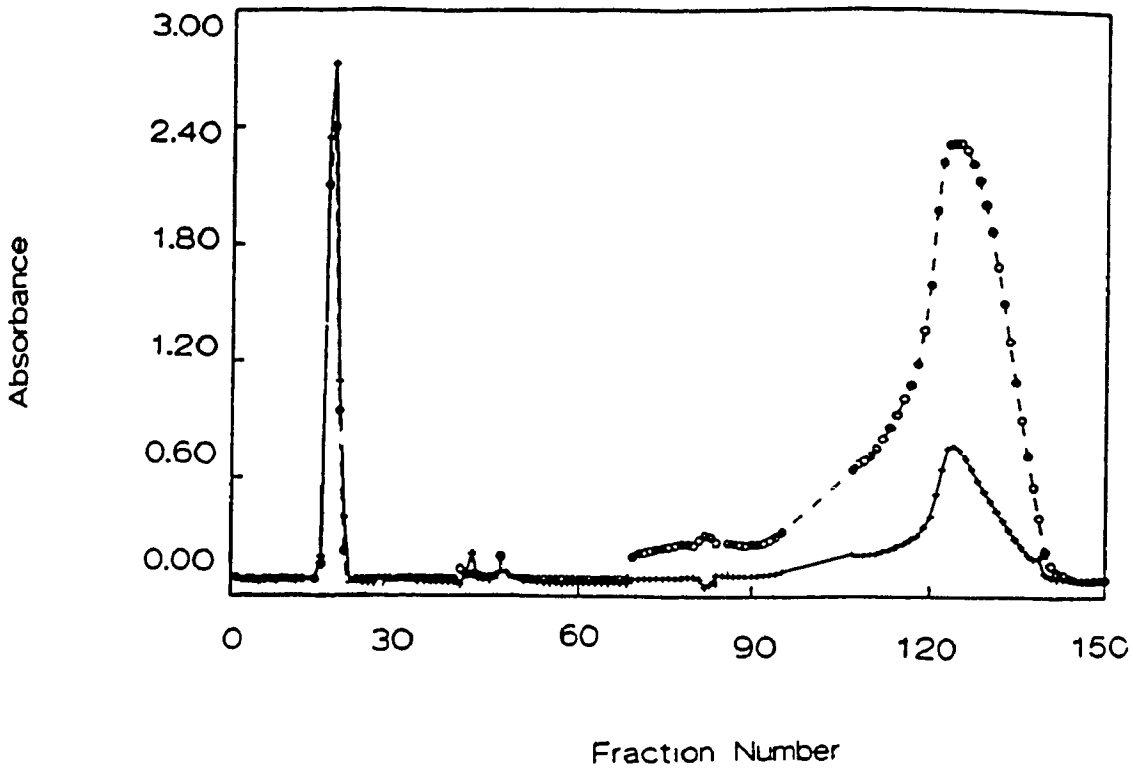

Figure 4.3: Large scale purification of cyt c (50 mg/ml) by cation-exchange (CM-Sepharose) chromatography. The column size was 1.5 x 60 cm. The eluent was 100 mM phosphate buffer, pH 7.0 at 4 °C, and the flow rate was 25 ml/hr. Absorbance was measured for each 10 ml fraction at 280 nm (+) and 410 nm (O).

ferricyanide, and the native form of cyt c was eluted in fractions 120 to 150.

4.2.2.3 Spectrophotometric Study of GOx Cyt c-Reducing Activity: The reduction of cyt c was investigated by measuring the change in absorbance at 550 nm ($\Delta\epsilon$ = 18.5 $mM^{-1}cm^{-1}$)[19]. A stock solution of ferricyt c with an A_{550} of ~ 0.5 was prepared in 0.1 M phosphate buffer, pH 7.0 and also in 0.1 M and 0.01 M bis-tris buffer, pH 7.0 under deaerated conditions. Stock solutions of 10 mg/ml GOx were made in the same buffers stock and diluted to 40 nM (total volume 2 ml) to which 55 mM glucose was added. The GOx solution was deaerated using N_2 gas and 500 µl of the GOx solution were added to 500 µl of the cyt c stock solution, and the absorbance was monitored at 550 nm for 5 min.

4.2.2.4 Modification of Au electrode : Immediately prior to use, the electrode was polished with 6 µM diamond polish for 15 min, rinsed with distilled water, and cycled in 1 M H_2SO_4 between - 0.300 V and + 1.550 V (vs Ag/AgCl) at a scan rate of 100 mV/s for 20 cycles or until a cyclic voltammogram corresponding to that of bare gold was obtained[20]. The electrode was rinsed and promoter chemisorption was carried out by immersion of the electrode into a 4 mM solution of the promoter for 15 min.

4.2.2.5 Electrochemistry of Cyt c at Au modified electrode: The same three-electrode cell configuration described in Section 3.2.2.6 was used except that for this experiment the working electrode was an Au electrode (surface area 0.0201 cm^2) that had been modified with a promoter. The potential was cycled between 250 and -150 mV at a scan rate of 20 mV/s. The cyt c solution was deoxygenated using a gentle stream of N_2 over the solution, and 1 M $NaClO_4$ was added as the supporting electrolyte.

4.2.2.6 Mediation of GOx Activity by Cyt c: This was carried out using the same

experimental setup given in the previous section. Ferricyt c and the supporting electrolyte were added to the electrochemical cell and the cyclic voltammogram of cyt c was obtained at a scan rate of 2 mV/s. GOx was added to the cell (20 μM), reducing the cyt c concentration to 166 μM, and the cyclic voltammogram was again recorded at the same scan rate. Finally glucose was added in order to obtain the catalytic current.

4.2.2.7 Electrochemistry of Cyt c in Carbon Paste: Stearic acid (50 mg) was combined with 10 drops of mineral oil and the mixture was heated to 40 °C. Carbon powder (0.75 g) was added and mixed in. Cyt c (1.6 μmol to 27.4 nmol) was added to the paste just before it was packed into an electrode holder and polished to a smooth finish. The potential was scanned between 150 and 800 mV and the scan rate was 20 mV/s.

4.2.2.8 Electrochemistry of Cyt c on Pyrolytic Carbon: Cyt c and $NaClO_4$ were added to the electrochemical cell to a final concentration of 250 μM and 0.5 M, respectively. The potential was scanned between -250 and 250 mV at a scan rate of 5 mV/s. The cyclic voltammograms were recorded at times 0, 10 and 20 min

4.3 Results

4.3.1 Spectrophotometric Study of GOx Cyt c-Reducing Activity: In 0.1 M phosphate buffer, pH 7.0, no change of absorbance at 550 nm was observed vs time for a solution containing ferricyt c, GOx and glucose When dithionite was added to this solution the absorbance at 550 nm increased immediately, indicating that the heme in cyt c can be reduced. In 10 mM phosphate buffer again no change in absorbance at 550 nm was observed over 5 min but the absorbance also increased upon addition of dithionite. Figure 4 4 (a) and (b) shows the results obtained when 0 1 M and 0.01 M deaerated bis-tris buffer, pH 7.0 were

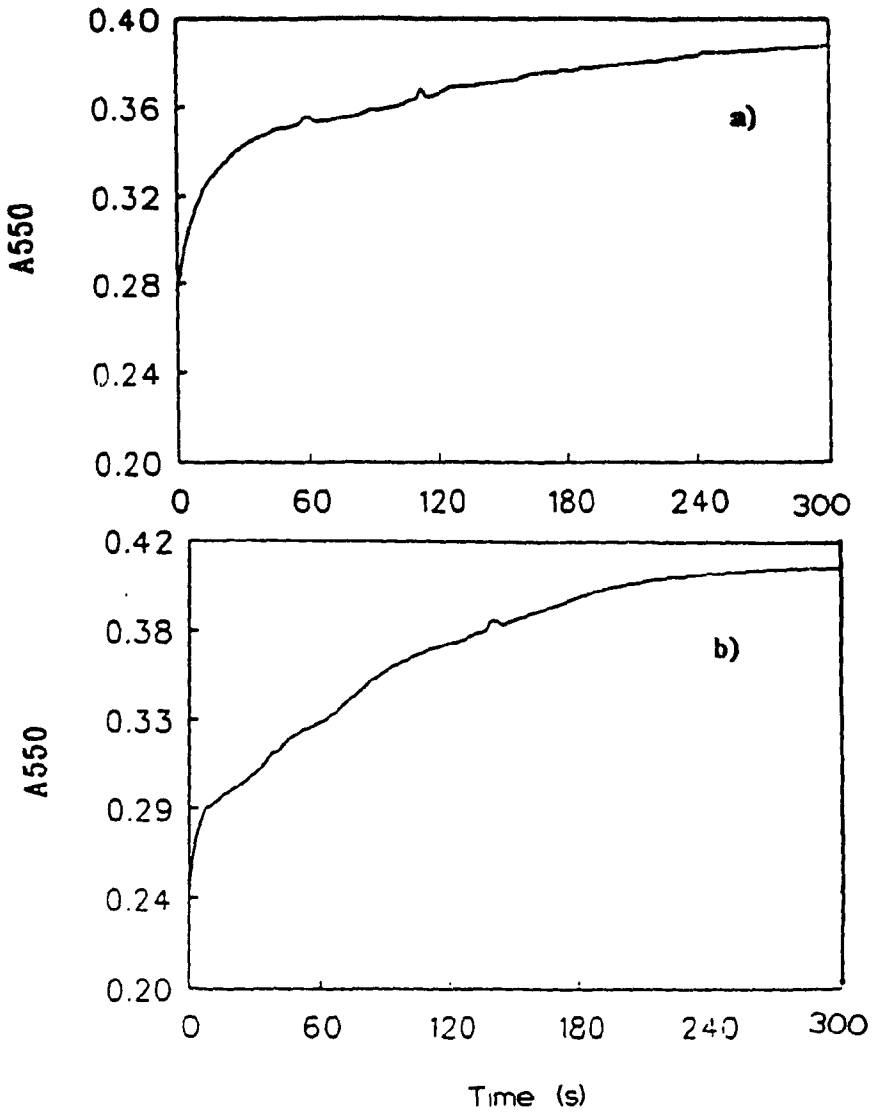

Figure 4.4: Spectrophotometric study of GOx oxidation by cyt c in a) 0.1 M bis-tris, pH 7 0 and b) 0.01 M bis-tris, pH 7.0. The concentrations of GOx in all samples was 20 nM and glucose 55 mM. Cyt c was taken from a stock solution with an initial absorbance of 0.5 which was purged with N_2. The absorbance was followed at 550 nm and the volume in the cuvette was 1.0 ml.

used, respectively. A change in absorbance at 550 nm was observed in both these buffers but a control containing no GOx did not exhibit an absorbance change.

From Figure 4.4 it appears that ferricyt c is a poor substrate for GOx. Reduction of the 27 μM ferricyt c used in the assay solution should give rise to an increase in absorbance at 550 nm from 0.25 to 0.76. However, as can be seen from Figure 4.4 after 5 min the absorbance at 550 nm is only ~0.4. Furthermore the absorbance increase with time is not linear which suggests that at 27 μM cyt c the enzyme may not be saturated with this substrate. Because of its high molar absorptivity it is not feasible to use mM concentrations of cyt c, which would also give rise to viscous solutions.

4.3.2 Mediation of GOx Activity by Cyt c: The Au electrodes were polished and cycled in 1 M H_2SO_4 before being modified with either L-Cys or 3-mercaptopropionic acid. The cyclic voltammogram obtained for a clean bare gold electrode surface in acid is shown in Figure 4 5. The voltammogram obtained for a Cys-modified Au electrode in 0.01 M bis-tris buffer, pH 7.0 is shown in Figure 4 6 (a) and that obtained when the electrode was placed in a 250 μM cyt c solution with supporting electrolyte is shown in Figure 4.6 (b), and Figure 4.6 (c) represents the same solution of cyt c after 20 μM GOx was added to it. The voltammogram observed upon addition of glucose is shown in Figure 4.6 (d), where the wave has the appearance of a catalytic voltammogram, but the magnitude of the current is very small

Large catalytic currents were not expected because cyt c was shown in the spectrophotometric assays to be a relatively poor electron-acceptor substrate for GOx. Nonetheless, in the electrochemical assays the concentration of cyt c was ~6-fold higher than

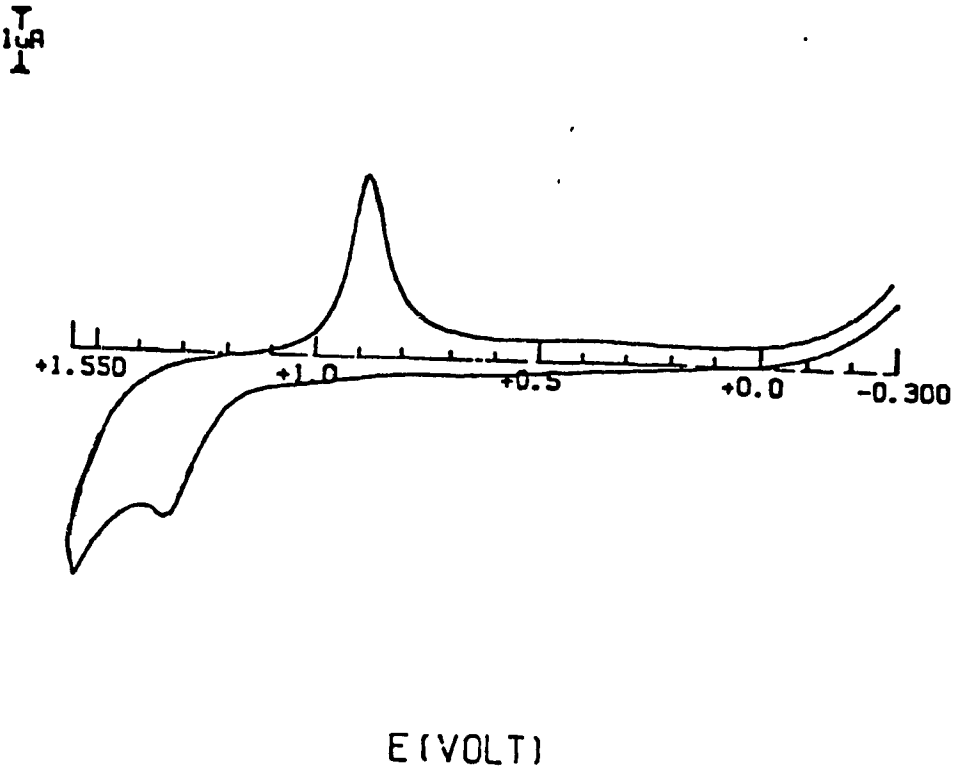

Figure 4.5: Cyclic voltammogram of an unmodified Au electrode obtained after polishing with 6 μm diamond polish for 15 minutes and rinsed with distilled water and cycled in 1 M H_2SO_4 between -0.300 V and + 1.500 V at a scan rate of 100 mV/s for 20 cycles.

Figure 4.6: Cyclic voltammograms of (a) Cys-modified Au electrode in bis-tris buffer , b) 250 μM cyt c with $NaClO_4$, c) after the addtion of 20 μM of GOx and in d) after addition of 55 mM glucose. The potential was scanned between 300 mV and -150 mV at a scan rate of 2 mV/sec.

a)

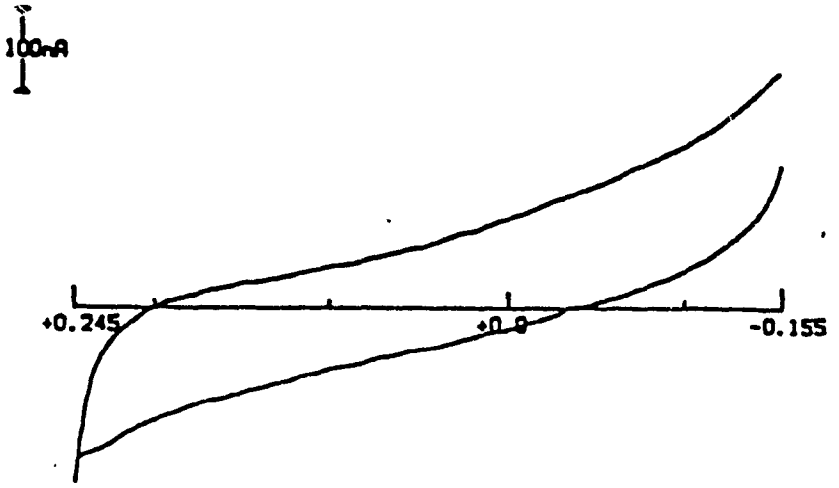

b)

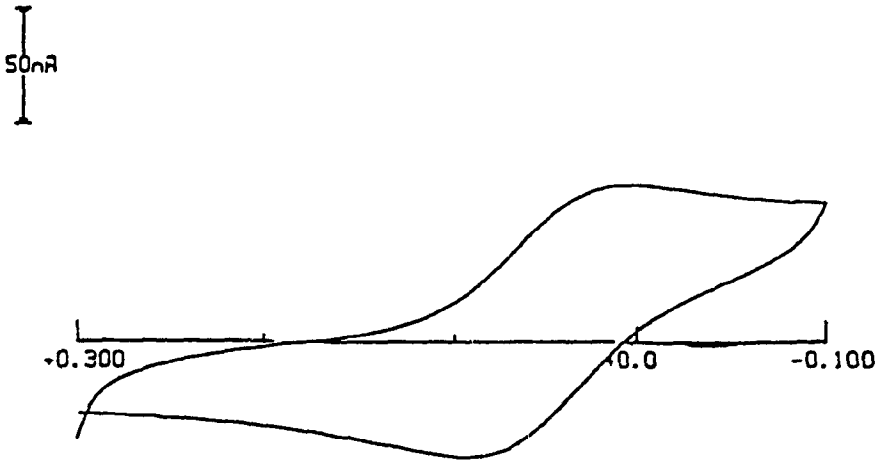

E(VOLT)

c)

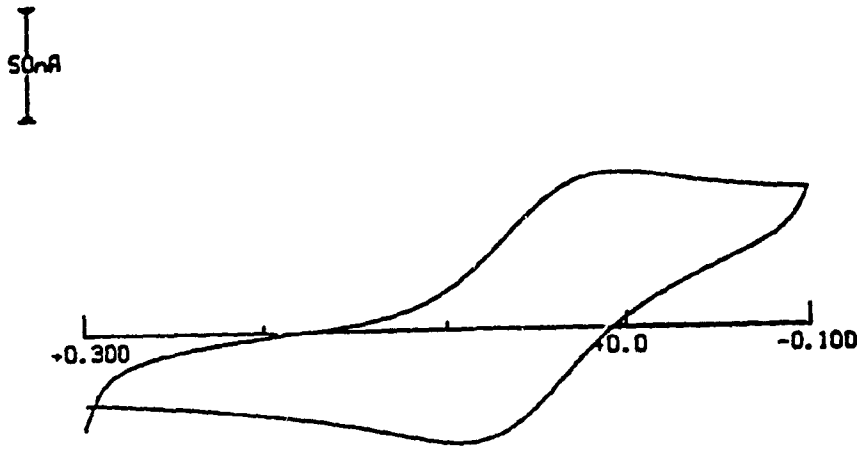

d)

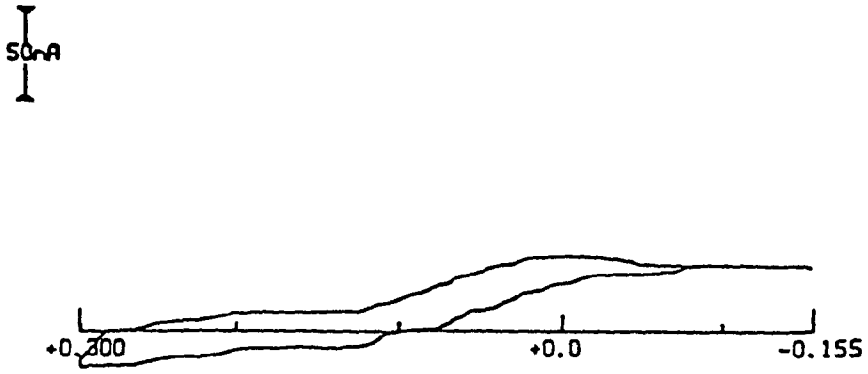

E(VOLT)

in the spectrophotometric assays, so current magnitudes larger than those observed were expected. To establish possible reasons for the low currents, studies on the stability of the modified electrodes were carried out. Three different Au electrodes that were modified with Cys were used to record the cyclic voltammograms of solutions containing 250 μM cyt c in 10 mM bis-tris with 1 M $NaClO_4$. The persistence of the cyt c signal at the three electrodes varied considerably. At one electrode a stable cyt c signal was observed for 24 h (Table 4.1), but the other two electrodes gave stable cyt c signals for only 15 min (Figure 4.7) and ~3 h.

Table 4.1: Catalytic peak current obtained for a Cys-modified Au electrode.

Time (Hour)	Cathodic peak current (10^{-7} A)[a]
0	1.02
0.5	1.26
1	1.04
1.5	1.05
24	1.20

[a] Experimental conditions: The potential was scanned between -150 to 250 mV at a scan rate of 20 mV/s. The supporting electrolyte was 1 M $NaClO_4$ and the concentration of cyt c was 250 μM.

However, with the most stable electrode a decrease in the cyt c signal was observed immediately following the addition of 55 mM glucose (Figure 4.8). The peak magnitudes are lower and also the peak separation is greater in the presence of glucose, indicating that cyt c electrochemistry at the Cys-modified Au electrode is less reversible when glucose is

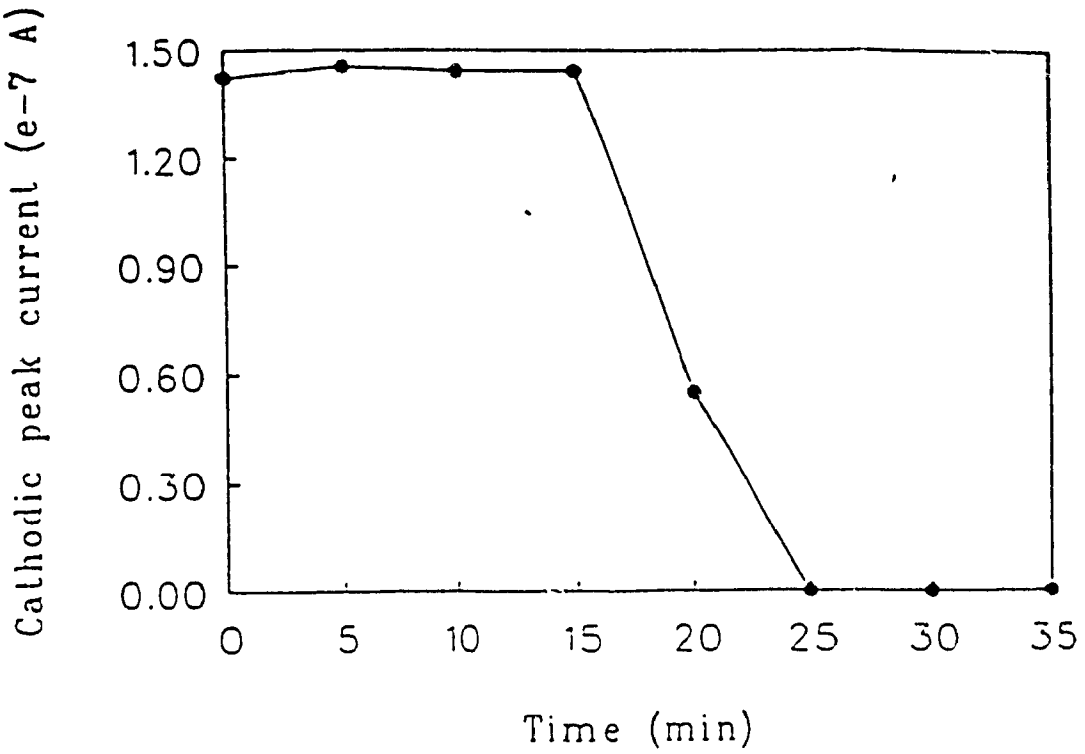

Figure 4.7: Plot of cathodic current vs time at a Cys-modified Au electrode obtained by voltammetry between 250 mV to -150 mV at a scan rate of 2 mV/s In all samples the concentration of cyt c was 250 μM. The supporting electrolyte was 1 M $NaClO_4$

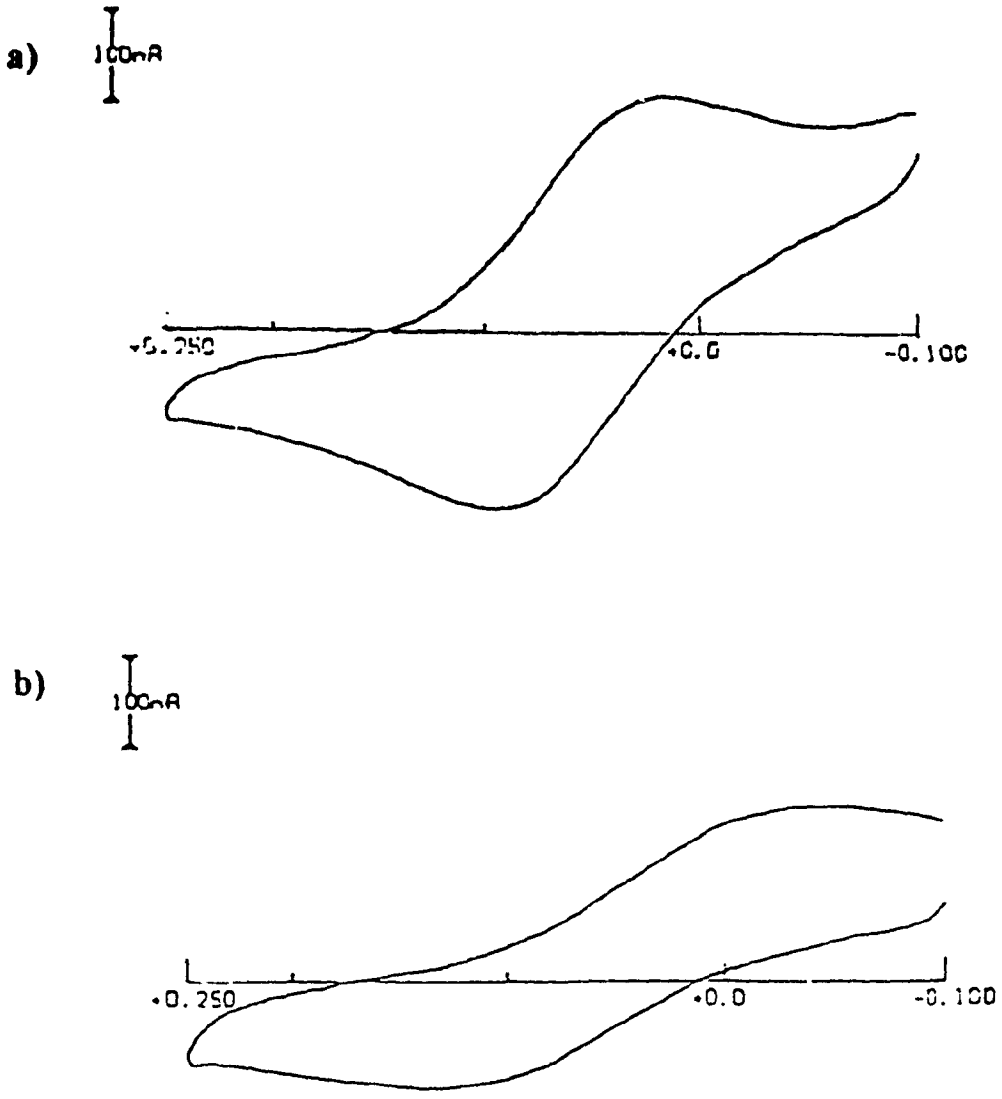

Figure 4.8: Cyclic voltamograms obtained with a Cys-modified Au electrode when 55 mM of glucose was added to 250 µM of cyt c The potential was scanned between -100 and 250 mV at a scan rate of 20 mV/sec

added. This would explain in part the low catalytic currents observed in the electrochemical assays of GOx using cyt c as an electron mediator

Cyt c electrochemistry was also investigated using carbon paste and pyrolytic carbon electrodes, and the voltammograms are shown in Figure 4.9. No significant signal was obtained with the carbon paste electrode, which contained a concentration of cyt c of 1.6 mM. A signal was observed with the pyrolytic carbon electrode but it showed a lot of resistance even in the presence of 1 M $NaClO_4$.

4.4 Discussion

In phosphate buffers the reduction of cyt c by glucose is not catalysed by GOx As mentioned in the previous section, dithionite was added to verify that cyt c was redox-active and the rapid increase in absorbance at 550 nm showed that cyt c could be readily reduced The inhibition of electron transfer between ferricyt c and reduced GOx in phosphate buffers may be due to phosphate binding to the cytochrome Cyt c is known to possess phosphate binding sites and when these sites are occupied its interaction with the negatively-charged GOx molecule is likely to be reduced. To eliminate phosphate binding, the activities were measured in bis-tris buffers and the results showed that ferricyt c can function as an electron-acceptor substrate for GOx. However, the slow nonlinear rate of cyt c reduction observed in Figure 4.4 sugests that at practical cyt c concentrations for a spectrophotometric assay ($\leq$ 50 μM) GOx is not saturated with cyt c.

In the electrochemical GOx assays with cyt c as mediator two factors were found to affect the magnitude of the currents measured at Cys-modified Au electrodes One factor was the stability of the modified electrode over time and the second was the interference of

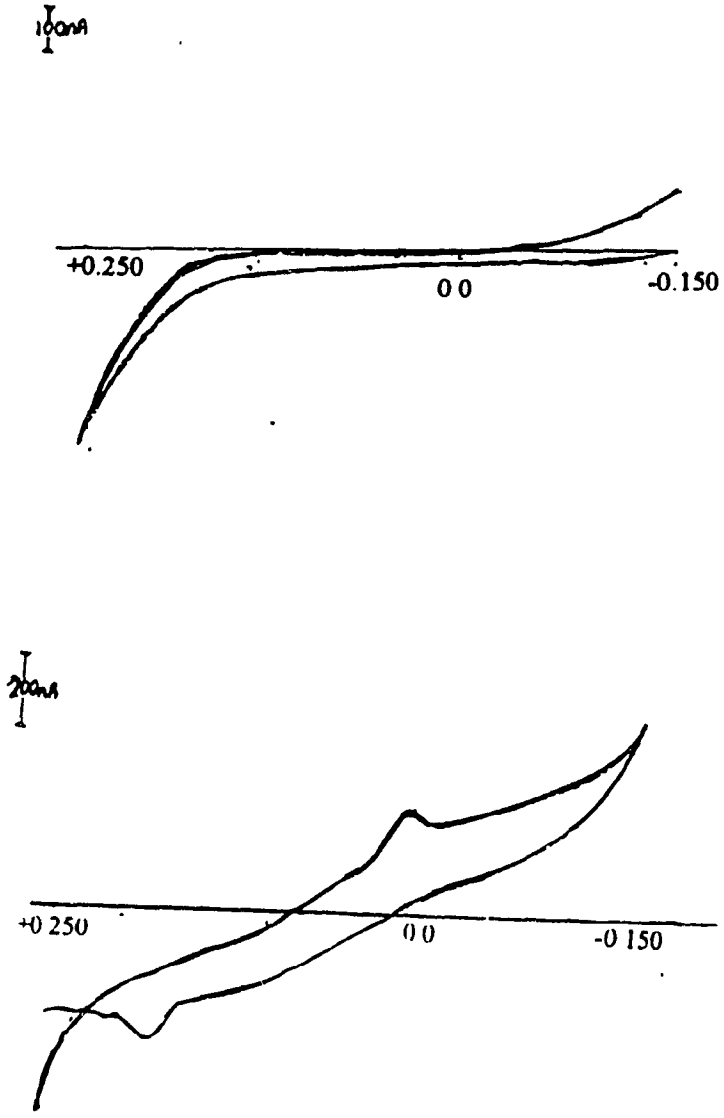

Figure 4.9: Cyclic voltammogram of (a) 1 6 mM cyt c in a carbon paste electrode. The potential was scanned between -150 and 800 mV at a scan rate of 20 mV/s, and (b) 250 μM cyt c in presence of supporting electrolyte at a basal-plane graphite electrode where the potential was scanned between -250 to 250 mV at scan rate of 5 mV/s

glucose with cyt c electrochemistry. Glucose must interact either with cyt c in solution or with the electrode surface in a manner that slows heterogeneous electron transfer Further studies are required to determine the nature of glucose interference with cyt c electrochemistry.

It has been shown that pre-activating the Au electrode surface with 4,4'-dithiodipyridine followed by polishing enhanced the persistence of the cyt c signal[6]. However, it is not known if this pretreatment would prevent glucose interference with cyt c electrochemistry. It should also be determined if the 3-mercaptopropionic acid electrodes are susceptible to glucose interference. Further work on the electrochemistry of cyt c in carbon paste and at pyrolytic graphite electrodes should be carried out to determine if suitable conditions can be found for reversible cyt c heterogenous electron transfer at these electrodes

GOx activity measured both spectrophotometrically and electrochemically using cyt c as a substrate yielded poor results Therefore, the effects of Ab binding on the cyt c-reducing activity of hapten-modified GOx was not investigated Considering the complications encountered in the approach taken in this thesis to enzyme amplified amperometric immunoassay development, an alternative strategy is suggested Conjugation of the mediator, rather than the enzyme label, with hapten should cause a dramatic decrease in the electrochemical activity of the enzyme on Ab binding to the mediator-hapten conjugate In the presence of free hapten the conjugate will be released from the Ab resulting in an increase in enzyme activity.

4.5 References

1) Degani, Y ; Heller, A., J. Am. Chem Soc , **1987**, 91, 1285-1289

2) Badia, A.; Carlini, R.; Fernandez, A.; Battaglini, F.; Mikkelsen, S.R.; English, A.M., J. Am. Chem. Soc., **1993**, 115, 7053-7060.

3) Zakeeruddin, S.M.; Fraser, D.M.; Nazeeruddin, M-K.; Gratzel, M., J. Electroanal. Chem., **1993**, 253

4) Kulys, J.J.; Cenas, N.K., Biochim. Biophys. Acta, **1983**, 744, 57-63.

5) Battaglini, F.; Koutroumanis, M.; English, A.M.; Mikkelsen, S.R., Bioconjugate Chem , **1994**, 5, 430-435.

6) Allen, P.H.; Hill, H.A O.; Walton, N.J., J.Electroanal.Chem., **1984**, 178, 69.

7) Bowden, E F ; Hawkridge, F.M ; Blount, H.N., J Electroanal.Chem., **1984**, 161, 355.

8) Durliat, H.; Comtat, M , Anal.Chem., **1982**, 54, 856.

9) Yeh, P ; Kuwana, T , Chem Lett , **1977**, 1145.

10) Eddowes, M J ; Hill, H.A.O , J Chem.Soc., Chem.Commun., **1977**, 722.

11) Bancfroft, E E , Blount, H.N.; Hawkridge, F M., Biochem Biophys.Res Commun., **1981**, 101, 1331.

12) Bowden, E.F ; Hawkridge, J.F.; Chlebowski, J.F.; Bancroft, E.E.; Tharpe, C ; Blount, H.N., J. Am. Chem Soc., **1982**, 104, 7641.

13) Hill, H A.O , Page, D J.; Walton, N.J., J.Electroanal.Chem., **1986**, 208, 395.

14) Di Gleria, K.; Hill, H.A O ; Lowe, V.J.; Page, D.J., J.Electroanal Chem., **1986**, 213, 333.

15) Reed, D.E., Hawkridge, F.M., Anal.Chem., **1987**, 59.

16) Brautigan, D.L., Fergusson-Miller, S.; Margoliash, E., Methods Enzymol., **1978**, 53, 120.

17) Eddowes, M.J.; Hill, H.A.O.; Vosaki, J., Bioelectrochem. Bioenergetics, **1980**, 7, 527.

18) Armstrong, F.A., Probing Metaloproteins by Voltammetry, Structure Bonding, Springer-Verlag Berlin Heidelberg, **1990**, 72, 151.

19) Margoliash, E.; Frahwirt, N.; Wiener, E., Biochem. J., **1959**, 71, 570-572

20) Woods, R., Electroanalytical Chemistry, Ed., Bard A.J., Marcel Dekker, New York, **1976**, 10.

5.0 Summary

The results in Chapter 2 showed that commercial GOx contains free FAD which can easily be removed by G-25 gel-filtration. Two peaks were observed for commercial GOx on a HIC FPLC column, and both had GOx activity. However, following G-25 gel filtration one of the peak almost disappeared suggesting that the G-25 column removed a small MW species that was bound to a fraction of the commercial GOx.

The ratio of FGA to GOx (5·1) obtained in this work is comparable to the ratios obtained for daunomycin and dopamine modification, carried out in concurrent work in our laboratory[1]. This implies that ~5 of the 132 carboxylic acid residues of GOx can be modified using EDC-NHS promoted amide bond formation Lys residues on GOx were targeted with DNBA, but it was not possible to determine the ratio of DNBA to GOx using the iron-thiocyanate procedure used here. However, previous work in this laboratory showed that using under the same conditions the EDC-NHS procedure yielded GOx species modified at an average of 12 Lys residues with ferrocenecarboxylic acid[2].

Enzymatic deglycosylation of GOx was attempted and ES-MS analysis of the products indicated ~16% mass loss due to deglycosylation. SDS-PAGE analysis, on the other hand, indicated that the deglycosylation was much less efficient. Further work is required to reconcile the discrepancy in the results from these two techniques.

Trp fluorescence measurements on GOx and $(FGA)_5$-GOx under both native and denaturing conditions confirmed that FGA was covalently bound to the enzyme. The quenching should be relieved under denaturing conditions if FGA was not covalently bound to GOx because free FGA would not be an efficient quencher of Trp residues at the

concentration used (low μM).

FGA fluorescence was also investigated and it was shown that, on covalent binding FGA to GOx, there is a sharp decrease in quantum yield. Also, a red-shift was observed in the emission maximum of FGA on its binding to GOx. Titration of FGA fluorescence with anti-F revealed that the Ab bound to free FGA ~50-fold more tightly than to $(FGA)_5$-GOx. The latter should be very similar in structure to the immunogen against which the anti-F was raised so its low Ab binding is surprising.

The electrochemical activity did not decrease upon addition of anti-F to $(FGA)_5$-GOx at Ab concentrations in excess of the estimated kD. Therefore, it was concluded that Ab binding did not induce a conformational change in the enzyme to cause activity loss, nor did it obstruct the active site to small mediators such as FCOH Similar conclusions were reached following the addition of anti-D to $(DNBA)_x$-GOx. Conjugation of these haptens to dGOx should be carried out since it is possible that the carbohydrate on GOx may interfere with the Ab-Ag interaction.

The use of cyt c as an electron-acceptor substrate for GOx was investigated both spectrophotometrically and electrochemically. It was hoped that cyt c, a large positively-charged molecule, would give rise to differential GOx activity in the presence and absence of Ab. However, because of the poor homogeneous and heterogeneous activity of GOx with cyt c, it was not considered a suitable substrate for immunoassay development One of the problems encountered in the electrochemical assay was the inhibition by glucose of cyt c electrochemistry at Cys-modified Au electrodes An alternative strategy for enzyme amplified amperometric biosensor development was suggested in Chapter 4

5.1 References

1) Battaglini, F.; Koutroumanis, M.; English, A.M.; Mikkelsen, S.R., Bioconjugate Chem., **1994**, 5, 430-435.

2) Badia, A.; Carlini, R.; Fernandez, A.; Battaglini, F.; Mikkelsen, S.R.; English, A.M., J. Am. Chem. Soc., **1993**, 115, 7053-7060.